(12) INTERNATIONAL APPLICATION PUBLISHED UNDER THE PATENT COOPERATION TREATY (PCT)

(19) World Intellectual Property Organization
International Bureau

(43) International Publication Date
22 June 2017 (22.06.2017)

WIPO | PCT

(10) International Publication Number
WO 2017/106381 A1

(51) International Patent Classification:
C07K 14/62 (2006.01) *A61K 38/28* (2006.01)
C12N 15/17 (2006.01) *A61P 5/50* (2006.01)
C12N 15/63 (2006.01)

(21) International Application Number:
PCT/US2016/066714

(22) International Filing Date:
14 December 2016 (14.12.2016)

(25) Filing Language: English

(26) Publication Language: English

(30) Priority Data:
62/267,162 14 December 2015 (14.12.2015) US

(71) Applicant: **CASE WESTERN RESERVE UNIVERSITY** [US/US]; 10900 Euclid Avenue, Cleveland, Ohio 44106 (US).

(72) Inventor: **WEISS, Michael A.**; 70 Woodburn Drive, Moreland Hills, Ohio 44022 (US).

(74) Agents: **CUNNIFF, John J.** et al.; Hahn Loeser and Parks LLP, 200 Public Square, Suite 2800, Cleveland, Ohio 44114 (US).

(81) Designated States *(unless otherwise indicated, for every kind of national protection available)*: AE, AG, AL, AM, AO, AT, AU, AZ, BA, BB, BG, BH, BN, BR, BW, BY, BZ, CA, CH, CL, CN, CO, CR, CU, CZ, DE, DJ, DK, DM, DO, DZ, EC, EE, EG, ES, FI, GB, GD, GE, GH, GM, GT, HN, HR, HU, ID, IL, IN, IR, IS, JP, KE, KG, KH, KN, KP, KR, KW, KZ, LA, LC, LK, LR, LS, LU, LY, MA, MD, ME, MG, MK, MN, MW, MX, MY, MZ, NA, NG, NI, NO, NZ, OM, PA, PE, PG, PH, PL, PT, QA, RO, RS, RU, RW, SA, SC, SD, SE, SG, SK, SL, SM, ST, SV, SY, TH, TJ, TM, TN, TR, TT, TZ, UA, UG, US, UZ, VC, VN, ZA, ZM, ZW.

(84) Designated States *(unless otherwise indicated, for every kind of regional protection available)*: ARIPO (BW, GH, GM, KE, LR, LS, MW, MZ, NA, RW, SD, SL, ST, SZ, TZ, UG, ZM, ZW), Eurasian (AM, AZ, BY, KG, KZ, RU, TJ, TM), European (AL, AT, BE, BG, CH, CY, CZ, DE, DK, EE, ES, FI, FR, GB, GR, HR, HU, IE, IS, IT, LT, LU, LV, MC, MK, MT, NL, NO, PL, PT, RO, RS, SE, SI, SK, SM, TR), OAPI (BF, BJ, CF, CG, CI, CM, GA, GN, GQ, GW, KM, ML, MR, NE, SN, TD, TG).

Published:

— *with international search report (Art. 21(3))*

[Continued on next page]

(54) Title: IODINATED INSULIN ANALOGUES WITH FORESHORTENED SIGNALING

(57) Abstract: An insulin analogue comprises an insulin B-chain polypeptide sequence containing a 3-iodo-Tyrosine or (3,5)-di-iodo-Tyrosine at position B26 relative to the positions of a wild type insulin B chain and may additionally comprise a substitution at a position corresponding to position B29 relative to the positions of a wild type insulin B chain, selected from a standard or non-standard amino-acid residue containing a neutral or acidic side chain. Position B29 may be Glu or Asp, or may be Ala, Leu, Ile, Val, aminoprioionic acid, aimnobutyric acid or Norleucine. The insulin analogue may be a two-chain or single-chain insulin analogue. The insulin analogue may be used to treat a patient with diabetes mellitus by administering a physiologically effective amount of the insulin analogue or a physiologically acceptable salt thereof to a patient by means of intravenous, intraperitoneal, or subcutaneous injection.

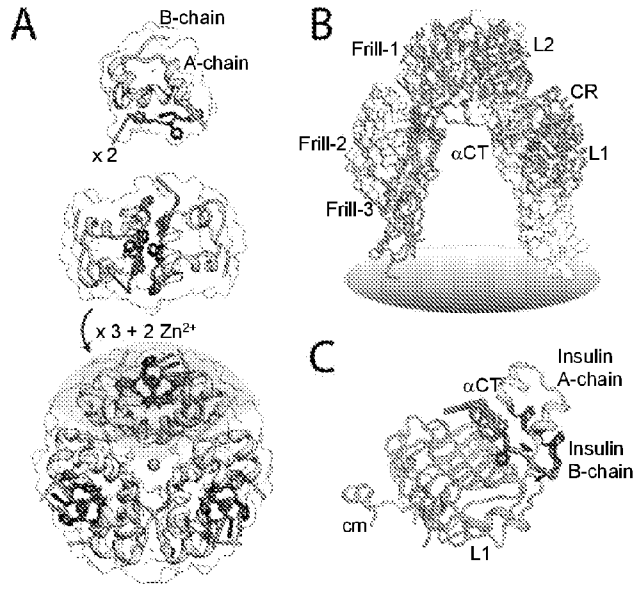

FIGURE 1
(Prior Art)

WO 2017/106381 A1

— *before the expiration of the time limit for amending the claims and to be republished in the event of receipt of amendments (Rule 48.2(h))*

— *with sequence listing part of description (Rule 5.2(a))*

IODINATED INSULIN ANALOGUES WITH FORESHORTENED SIGNALING

STATEMENT REGARDING FEDERALLY SPONSORED RESEARCH OR DEVELOPMENT

[0001] This invention was made with government support under grant numbers DK040949 and DK074176 awarded by the National Institutes of Health. The U.S. government has certain rights in the invention.

BACKGROUND OF THE INVENTION

[0002] This invention relates to polypeptide hormone analogues that exhibit enhanced pharmaceutical properties, such as improved stability (i.e., conferring extended shelf life or augmented resistance to degradation in a device reservoir, for example) and altered pharmacokinetic and pharmacodynamic properties (i.e., conferring accelerated absorption of the hormone from a subcutaneous depot or foreshortened duration of action relative to soluble formulations of the corresponding wild-type human hormone, for example). More particularly, this invention relates to derivatives of such insulin analogues containing one or more iodine atoms in the aromatic ring of Tyrosine at position B26 of the B chain in conjuction with (i) a neutral or acidic residue at position B29, optionally (ii) one or more A- or B-chain substitutions known in the art to foreshorten the duration of action of an insulin analogue once in the blood stream, and optionally (iii) one or more A- or B-chain substitutions or B-chain extensions known in the art to reduce binding of the insulin analogue to the Type 1 IGF-I receptor (IGF-1R). The insulins analogues of the present invention may optionally contain a connecting domain (C domain) between A- and B-chains (and so be described as single-chain analogues) and may optionally contain standard or non-standard amino-acid substitutions at other sites in the A- or B chains.

[0003] The engineering of proteins, including therapeutic agents and vaccines, may have broad medical and societal benefits. Naturally occurring proteins—as encoded in the genomes of human beings, other mammals, vertebrate organisms, invertebrate organisms, or eukaryotic cells in general—often contain two or more functional surfaces. A benefit of protein analogues would be to achieve selective

modification of one or the other of these functional surfaces, such as to provide fine-tuning of their thermodynamic stabilities, modes of self-assembly, and susceptibility to physical or chemical degradation. An example of a therapeutic protein is provided by insulin.

[0004] The three-dimensional structure of wild-type insulin has been well characterized as a zinc hexamer, as a zinc-free dimer, and as an isolated monomer in solution (Fig. 1A). Wild-type human insulin and insulin molecules encoded in the genomes of other mammals bind to insulin receptors (IRs), each of which containing multiple domains and associated domain surfaces (Fig. 1B). The IR is a dimer of αβ half-receptors (designated $(\alpha\beta)_2$) wherein the α chain and β chain are the post-translational products of a single precursor polypeptide. The hormone-binding surfaces of the $(\alpha\beta)_2$ dimer has been classified as *Site 1* and *Site 2* in relation to the non-linear binding and kinetic properties of the receptor. Recent advances in structural and biochemical analysis of fragments of the IR ectodomain have shown that Site 1 consists of a *trans*-binding element formed by both a subunits in the $(\alpha\beta)_2$ dimer: the N-terminal L1 domain of one subunit and the C-terminal α-helix (αCT) of the other.

[0005] The location of Site 2 is not well characterized but is proposed to comprise parts of the first and second fibronectin-homology domains. The receptor-binding surfaces of insulin or insulin analogues may likewise be classified on a cognate basis: the respective Site-1-binding surface (classical receptor-binding surface) and Site 2-binding surface (non-classical receptor-binding surface). The Site-1-binding surface of insulin overlaps its dimer-forming interface in the B chain whereas the Site-2-binding surface overlaps its hexamer-forming interface. The Site 1 hormone-IR interface has recently been visualized at low resolution as shown in Figure 2.

[0006] It is known in the art that substitution of Tyrosine at position B26 by 3-iodo-Tyrosine or (3,5)-di-iodo-Tyrosine of wild-type insulin leads to a small enhancement of affinity of the modified insulin for the insulin receptor. The degree of enhanced affinity is of a magnitude not associated with a change in biological potency in a mammal nor is such enhancement ordinarily associated with a foreshortening of

the pharmacodynamics of insulin signaling and in particular the duration of action once the hormone-receptor is engaged at target tissues. It was therefore unexpected to discover that this modification, when combined with appropriate substitutions at B29, can markedly foreshorten the duration of insulin action in a diabetic mammal relative to a control analogue (insulin *lispro*). The surprising nature of the present invention is highlighted by the absence of such foreshortening when 3-iodo-Tyr^{B26} is combined with the paired substitutions Pro^{B28}→Lys and Pro→Lys^{B29} (the active component of Humalog®). Likewise, an acidic substitution at position B29 by itself does not cause foreshortening of insulin action in a diabetic mammal. Further, substitution of Lysine B28 by Glutamic Acid in conjunction with an unmodified Tyrosine at position B26 is known in the art as a component of insulin glulisine (the active component of Apidra®) wherein Glutamic Acid at B28 is combined with the substitution of the naturally occurring Asparagine at position B3 by Lysine). This combination of substitutions at B3 and B28 recaptures the activity of wild-type insulin and does not confer the foreshortened signaling properties described in the present provisional application. The present invention thus has no precedents in past studies of insulin analogues and reflects a novel outcome of the paired modifications at positions B26 and B28.

[0007] Administration of insulin has long been established as a treatment for diabetes mellitus. A major goal of conventional insulin replacement therapy in patients with diabetes mellitus is tight control of the blood glucose concentration to prevent its excursion above or below the normal range characteristic of healthy human subjects. Excursions below the normal range are associated with immediate adrenergic or neuroglycopenic symptoms, which in severe episodes lead to convulsions, coma, and death. Excursions above the normal range are associated with increased long-term risk of microvascular disease, including retinapathy, blindness, and renal failure. Insulin is a small globular protein that plays a central role in metabolism in vertebrates. Insulin contains two chains, an A chain, containing 21 residues, and a B chain containing 30 residues; individual residues are indicated by the identity of the amino acid (typically using a standard three-letter code), the chain and sequence position (typically as a superscript). The hormone is stored in the

pancreatic β-cell as a Zn^{2+}-stabilized hexamer, but functions as a Zn^{2+}-free monomer in the bloodstream.

[0008] Insulin is the product of a single-chain precursor, proinsulin, in which a connecting region (35 residues) links the C-terminal residue of B chain (residue B30) to the N-terminal residue of the A chain. A variety of evidence indicates that it consists of an insulin-like core and disordered connecting peptide. Formation of three specific disulfide bridges (A6–A11, A7–B7, and A20–B19; Fig. 1A) is thought to be coupled to oxidative folding of proinsulin in the rough endoplasmic reticulum (ER). Proinsulin assembles to form soluble Zn^{2+}-coordinated hexamers shortly after export from ER to the Golgi apparatus. Endoproteolytic digestion and conversion to insulin occurs in immature secretory granules followed by morphological condensation. Crystalline arrays of zinc insulin hexamers within mature storage granules have been visualized by electron microscopy (EM).

[0009] Safe and effective glycemic control by regimens of insulin-replacement therapy benefit in general from insulin formulations or insulin analogue formulations that differ in speed of onset and duration of action. Rapid-acting insulin analogue formulations, for example, are more effective than long-acting insulin formulations (such as NPH insulin, Levemir® and Lantus®) for the control of glycemic excursions after meals. Rapid-acting insulin analogue formulations are also preferred for use in insulin pumps (continuous subcutaneous insulin infusion; CSII). Molecular strategies for the design of rapid-acting insulin analogues have to date focused on *pharmacokinetics* based on the rate of absorption of the insulin analogue from the subcutaneous depot. Such analogues (as exemplified by Apidra®, Humalog® and Novolog®) thus contain amino-acid substitutions that hasten the rate of disassembly of native insulin dimers, tetramers, and hexamers to facilitate SQ absorption into the blood stream. These products do not exhibit pharmacodynamics differences from wild-type insulin once circulating in the blood stream or once engaged at target tissues. The resulting tail of insulin action 3-5 hours after a meal thus exposes patients to the risk of hypoglycemia and also to weight gain consequent to the snacking that is often required to defend against hypoglycemia. In the context of an algorithm-controlled insulin pump coupled to a continuous glucose monitor (designated a

"closed-loop system), foreshortening of the duration of insulin signaling would also be expected to enhance the safety and robustness of the feedback algorithm. There is a need for an insulin analogue with a foreshortened duration of inulin signaling.

SUMMARY OF THE INVENTION

[0010] It is therefore an aspect of the present invention to demonstrate, as a novel pharmacologic principle, that an insulin molecule may be engineered to enhance the safety and efficacy of insulin analogue formulations by foreshortening the duration of insulin signaling in a diabetic mammal.

[0011] It is another aspect of the present invention to attenuate the tail of insulin signaling in a vertebrate organism following subcutaneous (SQ) or intravenous (IV) injection through the simultaneous modification of (i) the naturally occurring Tyrosine at position B26 of the B chain by mono-iodo-3-Tyrosine or di-iodo-(3,5)-Tyrosine and (ii) substitution of the naturally occurring Lysine at B28 of the B chain by an amino-acid residue with a neutral or acidic side chain. Such iodo-aromatic derivatives of rapid-acting insulin analogues promise to facilitate their safe and effective use in the treatment of diabetes mellitus following subcutaneous injection as a method of treatment of diabetes mellitus and of further utility in the algorithm-based operation of closed-loop systems for the treatment of diabetes mellitus ("smart pumps"), including use within both external and implantable intraperitoneal pumps.

[0012] The present invention focuses on Tyrosine at position B26 of the B chain in conjuction with substitutions of the naturally occurring Lysine at position B28 of the B chain. Residue B26 is part of the dimer-forming surface of insulin and so is presumed to contact in Site 1 near its edge (Fig. 2). This presumption is supported by residue-specific photo-cross-linking studies of a photo-activatable insulin derivative containing *para*-azido-Phenylalanine at position B26. Residue B28 is at the periphery of the receptor-binding surface of insulin, but its substitution by residues with neutral or acidic side chains attenuates cross-binding to IGF-1R.

[0013] The 3-I-Tyr^{B26} derivative of insulin, when paired with Norleucine at position B29, exhibits a remarkable and unexpected foreshortening of insulin action in a rat model of diabetes mellitus. It is envisaged that the 3-I-Tyr^{B26} (3,5)-I-Tyr^{B26}

derivatives of a broad class of insulin analogues in which the side chain at position B29 is neutral or acidic would confer similar benefits.

[0014] It is, therefore, an aspect of the present invention to provide two-chain and single-chain insulin analogues that provide foreshortened duration of insulin signaling due to substitution of Tyrosine at position B26 by 3-iodo-Tyrosine or (3,5)-di-iodo-Tyrosine in combination with a neutral or acidic amino-acid substitution at position B29. The analogues of the present invention contain at least a portion of the biological activity of wild-type insulin to direct an initial reduction in the blood glucose concentration on subcutaneous or intravenous injection.

[0015] In the following the following abbreviations are used: 3-I-Tyr^{B26}-KP-insulin, insulin analogue containing 3-iodo-Tyrosine at position B26 of insulin *lispro*; CD, circular dichroism; HPLC, high-performance liquid chromatography; KP-insulin, analogue containing substitutions Pro^{B28}→Lys and Lys^{B29}→Pro; terpy, 2,2':6',2"-terpyridine; ThT, thioflavin T; and TR transition, conformational equilibria among zinc-stabilized insulin hexamers types T_6, $T_3R^f_3$, and R_6 (R^f, frayed R state). Amino acids are designated by standard one- and three-letter codes.

BRIEF DESCRIPTION OF THE SEVERAL VIEWS OF THE DRAWINGS

[0016] Figure *1* is a series of panels illustrating the structure of insulin and the ectodomain of the IR. (Panel *A*) Assembly of the zinc insulin coordinated WT hexamer. The insulin monomer (A- and B chains) forms zinc-free dimers *via* anti-parallel association of B-chain α-helices and C-terminal β-strands (dark); two zinc ions then mediate assembly of three dimers to form classical hexamer (T_6). The A chain is shown as grey ribbon, and the B chain in light gray (B1-B19) or dark gray(B20-B30). The conserved aromatic residues of Phe^{B24} and Phe^{B25} are shown as black sticks whereas Tyr^{B26} is dark gray. (Panel *B*) Inverted V-shaped assembly of IR ectodomain homodimer. One monomer is in ribbon representation (*labeled*), the second in surface representation. Domains are labeled as follows: L1, first Leu-rich repeat domain; CR, Cys-rich domain; L2, second Leu-rich repeat domain; FnIII-1,-2 and -3, first, second and third fibronectin Type III domains, respectively; and αCT: α-chain C-terminal segment. (Panel *C*) Model of WT insulin in its receptor-free

conformation overlaid onto the structure of the insulin-bound μIR as described by Menting and colleagues (above). L1 and part of CR are shown in dark gray; αCT is shown in light gray. Residues Phe^{B24}, Phe^{B25} and Tyr^{B26} are as in panel A. The B chain of μIR-bound insulin is shown in black (B6-B19); the dark gray tube indicates classical location within the overlay of residues B20-B30 of insulin in its receptor-free conformation, highlighting steric clash of B26-B30 with αCT. Coordinates were obtained from PDB entries 4INS, 3LOH, and 3W11.

[0017] Figure *2* is a series of panels illustrating the insulin sequence and μIR complex. (Panel *A*) Sequence of WT insulin and sites of modification. A- and B chains are shown in white (SEQ ID NO: 2) and gray (SEQ ID NO: 3). Conserved aromatic residues Phe^{B24} and Phe^{B25} are highlighted as black circles. The present study focused on substitutions of Tyr^{B26} (marked with asterisk); additional substitutions were made at position B29 (Nle or Orn; encircled X) to facilitate semi-synthesis. (Panel *B*) Stick representation of residues B20-B27 (carbon atoms (*medium gray ribbon*), nitrogen atoms (*dark gray ribbon*) and oxygen atoms (*dark gray end points*) packed between αCT and the L1-β_2 sheet. B-chain residues B8-B19 are shown as a *black* ribbon and the A chain as a *light gray* ribbon; residues A1-A3 are concealed behind the surface of αCT. Key contact surfaces of αCT with B24-B26 are highlighted in *light gray surface structure*, and of L1 with B24-B26 are highlighted in *medium gray surface structure*; L1 and αCT surfaces not in interaction with B24-B26 are shown in lighter shades. (Panel *C*) Orthogonal view to (Panel *B*), showing interaction of the side chain of Phe^{B24} with the nonpolar surface of the L1-β_2 sheet. Tyr^{B26} is hidden below the surface of αCT. Engagement of conserved residues A1-A3 against the nonpolar surface of αCT is shown at top. (Panel *D*) Environment of Tyr^{B26} within Site 1 complex (stereo). Neighboring side chains in L1 and αCT are as labeled. Coordinates were obtained from PDB entry 4OGA.

[0018] Figure 3 is a pair of graphs showing results of functional screening of insulin analogs. (Panel *A*) Competitive receptor-binding assay of Orn^{B29}-insulin (*squares*; line indicates fitted model); its K_d is estimated to be 0.038(±0.006) nM. Model curves simulated based on K_d values that are 10-fold (*middle*) or 100-fold (*top*)

greater than that of Orn^{B29}-insulin are also shown. *Gray* dots indicate binding of insulin analogues Leu^{B26} (*top*), Met^{B26} (*middle*), and Gln^{B26} (*bottom*) at a concentration of 0.75 nM. Vertical axis: B/B_0 where B is ^{125}I-Tyr^{A14}-insulin bound by receptor at the designated insulin concentration and B_0 is ^{125}I-Tyr^{A14}-insulin bound by receptor in the absence of unlabeled insulin. (Panel *B*) Coarse screening at an analogue concentration of 0.75 nM. The analogues were classified as being of low, intermediate, or high affinity depending on the degree of ^{125}I-Tyr^{A14}-insulin displacement.

[0019] Figure *4* is a pair of graphs showing receptor isoform selectivity assay. Competitive displacement assays comparing Asn^{B26}-Orn^{B29}-insulin (*triangles*) and Gln^{B26}-Orn^{B29}-insulin (*open circles*) to their parent analogue Orn^{B29}-insulin (*squares*) in binding assays employing lectin-purified and detergent-solubilized IR-A (Panel A) or IR-B (B) as immobilized in a 96-plate well (see Experimental Procedures). Similar trends were observed with either receptor isoform. Analogue data represent mean of two replicates.

[0020] Figure *5* is a series of graphs showing studies of structure, stability and fibrillation. (Panel *A*) Far-UV CD spectra of Orn^{B29}-insulin (*medium gray*), Glu^{B26}-Orn^{B29}-insulin (*light gray*), Orn^{B26}-Orn^{B29}-insulin (*dark gray*) and Ser^{B26}-Orn^{B29} insulin (*black*) at neutral pH 7.4 and 25°C. Ellipticity was normalized per residue. (Panel *B*) Corresponding guanidine-unfolding transitions for samples in Panel A as monitored at 222 nm. Thermodynamic stabilities were derived using a two-state model (see Table 2). (Panels *C* and *D*) CD spectra and denaturation transitions of WT insulin (HI) (*black*), Orn^{B29}-insulin (*medium gray*), 3-I-Tyr^{B26}-Orn^{B29}-insulin (*light gray*). (Panels *E* and *F*) CD spectra and denaturation transitions of WT insulin (*black*), Nle^{B29}-insulin (*medium gray*) and 3-I-Tyr^{B26}-Nle^{B29}-insulin (*dark gray*). (Panel *G*) Histogram of ΔG_u values in kcal mol^{-1}. Marked changes in stability were evident depending on the identity of the substitution. (Panel *H*) Dot plot of lag time to fibril formation (days) of insulin analogs. Onset of fibrillation was defined by a two-fold enhancement of ThT fluorescence.

[0021] Figure *6.* Is a series of panels illustrating the crystal structure of the 3-I-Tyr^{B26} insulin analogue. (Panel *A*) Variant R_6 hexamer. A- and B chains are shown as

black and *medium gray* ribbons respectively. Iodine atoms are shown as large spheres (van der Waals radii). The two axial zinc ions are aligned at center (small center sphere), coordinated by threefold-related His^{B10} side chains (*light gray*). (Panel *C*) Stereo view of aromatic-rich dimer interface. The side chains of Tyr^{B16}, Phe^{B24}, Phe^{B25} and 3-I-Tyr^{B26} (*dark gray* sticks) are shown in relation to their dimer-related partners (indicated by primes) and a portion of the anti-parallel β-sheet (*light gray*; main chain of residues B24-B26 and B24'-B26'). The iodine atoms are shown as *gray* spheres. (Panel B) Superposition of WT protomer (*light gray*) and 3-I-Tyr^{B26} analogue (*dark gray*). Side chains of Tyr^{B26} and 3-I-Tyr^{B26} are shown as sticks. For clarity, the iodine atom is shown as a transparent *medium gray* sphere. (Panel *D*) Expanded view of corresponding WT and variant B26 side-chain environments in relation to an inter-chain crevice containing Ile^{A2}, Val^{A3} and Val^{B12}. Neighboring side chains are as labeled; the sulfur atoms of cystine A7-B7 are shown as *light gray* spheres (van der Waals radii). Wild type coordinates for panels *C* and *D* were obtained from PDB entry 1ZNJ.

[0022] Figure *7*. Is a series of panels showing crystallographic features of the R_6 3-I-Tyr^{B26} insulin analogue hexamer. (Panel *A*) ($2F_{obs}$-F_{calc}) difference electron density contoured at the 1σ level of a representative bound phenol molecule. Its *para*-OH group participates in hydrogen bonding with the carbonyl oxygen of Cys^{A6} and amide proton of Cys^{A11} (cystine A6-A11). An edge-to-face interaction occurs with the imidazole ring of His^{B5} from another dimer. (Panel *B*) Stereo view as in (Panel A) aligning the structure of the analogue (*dark gray*) with that of WT insulin as an R_6 hexamer (*light gray*). (Panel *C*) Electron density of 3-I-Tyr^{B26} and surrounding residues. (Panel *D*) Stereo view of residues seen in panel C (stick representation) superposed as in panel *B*. Coordinates for panels *B* and *D* were obtained from PDB entry 1ZNJ.

[0023] Figure *8* shows the side-chain arrangement within the respective dimer interfaces for residues B23-B26 within the crystal structure of (Panel A) the 3-I-Tyr^{B26}-Nle^{B29}-insulin hexamer and (Panel B) the WT insulin R_6 zinc hexamer (PDB

entry 1ZNJ). The three sub-panels within (A) and (B) correspond to the respective three copies of the dimer interface within the crystallographic asymmetric units of the two structures. Within each sub-panel, the side chain-carbon atoms of Phe^{B24} and its non-crystallographic symmetry equivalents are shown in *green*, of Phe^{B25} and its non-crystallographic symmetry equivalents in *dark gray* and of 3-I-Tyr^{B26} or Tyr^{B26} and their non-crystallographic symmetry equivalents in *medium gray*, while all backbone atoms are in *light gray,* as are the side-chain atoms of Thr^{B27} and its non-crystallographic symmetry equivalents. The *arrows* on the right assist in identifying the direction of the respective polypeptides within each sub-panel. Chains within each sub-panel correspond—from left to right—to chains B, D, F, H, J and L (respectively) within each structure. Overlaid on the three sub-panels in (Panel A) is σ_A-weighted ($2F_{obs}$-F_{calc}) difference electron density contoured at the 0.75 σ level and masked to within 2.5 Å of the side chain atoms of Phe^{B25} and its symmetry-related equivalents. The values displayed under the respective chains within the sub-panels of (Panel B) correspond to the side chain occupancies of the Phe^{B25} and its respective non-crystallographic symmetry equivalents within PDB entry 1ZNJ.

[0024] *Figure 9* is a series of graphs illustrating insulin activity in diabetic rats. Following IV bolus injection of insulin or an insulin analog, the time course of reduction and recovery of blood-glucose concentration is shown at *left*, and corresponding percentage reductions relative to the initial level of glycemia are shown at *right*. Labeling is as follows (Panels *A* and *B*) WT (*black circles,* N = 5), Orn^{B29}-insulin (*gray circles,* N = 5), Lys^{B28}-Pro^{B29}-insulin (*open squares*, N = 5). (Panels *C* and *D*) Orn^{B29}-insulin (*medium gray,* N = 4), Glu^{B26}-Orn^{B29}-insulin (*light gray*, N = 4), Ser^{B26}-Orn^{B29}-insulin (*dark gray*, N = 4). (Panels *E* and *F*) Orn^{B29}-insulin (*dark gray,* N = 5), Orn^{B26}-Orn^{B29}-insulin (*light gray*, N = 5). The dose administered was 10 µg of insulin analogue per 300 g rat; for WT insulin, this corresponds to 0.28 IU.

[0025] *Figure 10* is a series of panels showing pharmacodynamic parameters in rat studies. (Panel A) Time-dependent decrease and recovery of blood glucose concentration (*vertical axis*) on iv bolus injection of insulin analogs: Nle^{B29}-insulin

(*dark gray*, N = 20) and 3-I-Tyr^{B26}-Nle^{B29}-insulin (*light gray*, N = 18). Blood glucose measurements were obtained at indicated times (*horizontal axis*) with standard errors represented by *vertical bars*. (Panel B) Data normalized to initial blood glucose concentrations for Nle^{B29}-insulin (*con*), 3-I-Tyr^{B26}, Nle^{B29}-insulin (*I-con*) and wildtype (*WT*); *vertical axis* represents fraction of initial value. (Panel C) Initial rates of decrease in blood glucose over first hour in box plot representation. The *vertical scale* is change in blood glucose over the first hour (mg/dl/h). Each point represents the data obtained from one rat. Coloring is as above with the addition of *black* representing WT. *Vertical* bars represent values 50% greater than the inner quartile range. (Panel D) Same data as shown in C but in bar graph representation. No significant differences were seen between analogs. (Panel E) Data depicting calculated areas over the curve (AOC) over the first 80 min for Nle^{B29}-insulin and 3-I-Tyr^{B26}-Nle^{B29}-insulin in both bar graph (*left*) and box plot (*right*) representations. (Panel F) AOC over minutes 80 – 360 min for tested insulin analogs. Significant differences ($p < 0.05$) were seen between the iodinated analogue and control.

DETAILED DESCRIPTION OF THE INVENTION

[0026] The present invention is directed toward a two-chain or single-chain insulin analogue that provides foreshortened duration of action, a ratio of IR-A/IR-B receptor-binding affinities similar to that of wild-type insulin with absolute affinities in the range 5-100% (the lower limit chosen to correspond to proinsulin). The present invention may be combined with substitutions known in the art to confer unrelated properties or (as disclosed by the present inventor) foreshortening of insulin action by an unrelated molecular mechanism. An example of B-chain substitutions known in the art to confer rapid absorption is the combination of Lysine at position B3 and Glutamic Acid at position B29 when formulated in the absence of zinc ions. Amino-acid substitutions introduced previously by the present inventor to effect foreshortened duration of signaling may be at one or more of the following positions: B13, B17, A12, A13, and A17. These positions are regarded in the art as defining most or all of the "Site-2-related surface of insulin." Residue B26 of the present invention by contrast lies in the classical receptor-binding surface (also designated the

"Site-1-related surface of insulin"). Examples of such substitutions are provided by Tryptophan, Tyrosine, Alanine (except at B13), Histidine, Glutamic Acid (except at A17), and Glutamine. It is a feature of the present invention that the isoelectric point of the single-chain analogue is between 3.5 and 6.0 such that a soluble formulation neutral conditions (pH 6.8-8.0) would be feasible.

[0027] It is also envisioned that single-chain analogues may also be made with A- and B-domain sequences derived from animal insulins, such as porcine, bovine, equine, and canine insulins, by way of non-limiting examples. In addition or in the alternative, the insulin analogue of the present invention may contain a deletion of residues B1, B1 and B2, or B1-B3 or may be combined with a variant B chains modified by O-linked or N-linked saccharides (monosaccharides such as mannose, N-acetyl-galactose or glucose, disaccharides, or oligosaccharides). It is in particular envisioned that Thr^{B27}, Thr^{B30}, or one or more Serine residues in the C-domain may be modified, singly or in combination, by a monosaccaride adduct; examples are provided by O-linked N-acetyl-β-D-galactopyranoside (designated GalNAc-Oβ-Ser or GalNAc-Oβ-Thr), O-linked α-D-mannopyranoside (mannose-Oβ-Ser or mannose-Oβ-Thr), and/or α-D-glucopyranoside (glucose-Oβ-Ser or glucose-Oβ-Thr). The B-chain of two-chain analogues of the present invention, or the B-domain of the single-chain insulin analogues of the present invention, may optionally contain non-standard substitutions, such as D-amino-acids at positions B20 and/or B23 (intended to augment thermodynamic stability, receptor-binding affinity, and resistance to fibrillation), a halogen modification at the 2 ring position of Phe^{B24} (i.e., *ortho*-F-Phe^{B24}, *ortho*-Cl-Phe^{B24}, or *ortho*-Br-Phe^{B24}; intended to enhance thermodynamic stability and resistance to fibrillation), and/or 2-methyl ring modification of Phe^{B24} (intended to enhance receptor-binding affinity).

[0028] Furthermore, in view of the similarity between human and animal insulins, and use in the past of animal insulins in human patients with diabetes mellitus, it is also envisioned that other minor modifications in the sequence of insulin may be introduced, especially those substitutions considered "conservative." For example, additional substitutions of amino acids may be made within groups of amino acids with similar side chains, without departing from the present invention. These include

the neutral hydrophobic amino acids: Alanine (Ala or A), Valine (Val or V), Leucine (Leu or L), Isoleucine (Ile or I), Proline (Pro or P), Tryptophan (Trp or W), Phenylalanine (Phe or F) and Methionine (Met or M). Likewise, the neutral polar amino acids may be substituted for each other within their group of Glycine (Gly or G), Serine (Ser or S), Threonine (Thr or T), Tyrosine (Tyr or Y), Cysteine (Cys or C), Glutamine (Glu or Q), and Asparagine (Asn or N). Basic amino acids are considered to include Lysine (Lys or K), Arginine (Arg or R) and Histidine (His or H). Acidic amino acids are Aspartic acid (Asp or D) and Glutamic acid (Glu or E). Unless noted otherwise or wherever obvious from the context, the amino acids noted herein should be considered to be L-amino acids. Standard amino acids may also be substituted by non-standard amino acids belong to the same chemical class. By way of non-limiting example, the basic side chain Lys at position B29 may be replaced not only by standard amino acids containing aliphatic side chains (Alanine, Isoleucine, Leucine or Valine), but also by non-standard amino acids containing aliphatic side chains (Norleucine, aminobutyric acid, or aminopropionic acid). Residue B29 may also be substituted by Glutamic Acid or Aspartic Acid.

[0029] The amino-acid sequence of human proinsulin is provided, for comparative purposes, as SEQ ID NO: 1.

[0030] SEQ ID NO: 1 (human proinsulin)

Phe-Val-Asn-Gln-His-Leu-Cys-Gly-Ser-His-Leu-Val-Glu-Ala-Leu-Tyr-Leu-Val-Cys-Gly-Glu-Arg-Gly-Phe-Phe-Tyr-Thr-Pro-Lys-Thr-Arg-Arg-Glu-Ala-Glu-Asp-Leu-Gln-Val-Gly-Gln-Val-Glu-Leu-Gly-Gly-Gly-Pro-Gly-Ala-Gly-Ser-Leu-Gln-Pro-Leu-Ala-Leu-Glu-Gly-Ser-Leu-Gln-Lys-Arg-Gly-Ile-Val-Glu-Gln-Cys-Cys-Thr-Ser-Ile-Cys-Ser-Leu-Tyr-Gln-Leu-Glu-Asn-Tyr-Cys-Asn

[0031] The amino-acid sequence of the A chain of human insulin is provided as SEQ ID NO: 2.

SEQ ID NO: 2 (human A chain)

Gly-Ile-Val-Glu-Gln-Cys-Cys-Thr-Ser-Ile-Cys-Ser-Leu-Tyr-Gln-Leu-Glu-Asn-Tyr-Cys-Asn

[0032] The amino-acid sequence of the B chain of human insulin is provided as SEQ ID NO: 3.

SEQ ID NO: 3 (human B chain)

Phe-Val-Asn-Gln-His-Leu-Cys-Gly-Ser-His-Leu-Val-Glu-Ala-Leu-Tyr-Leu-Val-Cys-Gly-Glu-Arg-Gly-Phe-Phe-Tyr-Thr-Pro-Lys-Thr

[0033] SEQ ID NO: 4 (modified human B chain)

Phe-Val-Asn-Gln-His-Leu-Cys-Gly-Ser-His-Leu-Val-Glu-Ala-Leu-Tyr-Leu-Val-Cys-Gly-Glu-Arg-Gly-Phe-Phe-Xxx_1-Thr-Pro-Xxx_2-Thr

where Xxx_1 represents 3-iodo-Tyr or (3,5)-di-iodo-Tyr and where Xxx_2 represents an amino acid containing a neutral or acidic side chain.

[0034] SEQ ID NO: 5 (modified human B chain)

Phe-Val-Asn-Gln-His-Leu-Cys-Gly-Ser-His-Leu-Val-Glu-Ala-Leu-Tyr-Leu-Val-Cys-Gly-Glu-Arg-Gly-Phe-Phe-Xxx_1-Thr-Pro-Nle-Thr

where Xxx_1 represents 3-iodo-Tyr or (3,5)-di-iodo-Tyr and where Nle represents norleucine.

[0035] SEQ ID NO: 6 (modified human B chain)

Phe-Val-Asn-Gln-His-Leu-Cys-Gly-Ser-His-Leu-Val-Glu-Ala-Leu-Tyr-Leu-Val-Cys-Gly-Glu-Arg-Gly-Phe-Phe-Xxx_1-Thr-Xxx_2-Pro-Thr

where Xxx_1 represents 3-iodo-Tyr or (3,5)-di-iodo-Tyr and where Xxx_2 represents an amino acid containing a neutral or acidic side chain.

[0036] SEQ ID NO: 7 (modified human B chain)

Phe-Val-Asn-Gln-His-Leu-Cys-Gly-Ser-His-Leu-Val-Glu-Ala-Leu-Tyr-Leu-Val-Cys-Gly-Glu-Arg-Gly-Phe-Phe-Xxx_1-Thr-Nle-Pro-Thr

where Xxx_1 represents 3-iodo-Tyr or (3,5)-di-iodo-Tyr and where Nle represents norleucine.

EXPERIMENTAL PROCEDURES

[0037] *Preparation of Insulin Analogues*—Analogues were made by trypsin catalyzed semi-synthesis using an insulin fragment, *des*-octapeptide[B23-B30]-insulin and modified octapeptides as described (Pandyarajan, V., et al. *J. Biol. Chem.* **289**, 34709-27 (2104)). The *des*-octapeptide[B23-B30]-insulin was generated *via* cleavage of human insulin with trypsin and purified by reverse-phase high-performance liquid chromatography (HPLC); octapeptides were synthesized by solid-phase synthesis. The formation of a peptide bond between Arg^{B22} and a synthetic octapeptide was mediated by trypsin (in a mixed solvent system containing 1,4-butanediol and dimethylacetamide) as previously described. Insulin analogues were purified by preparative reverse-phase C4 HPLC (Higgins Analytical Inc, Proto 300 C4 10 μM, 250 x 20 mm), and their purity assessed by analytical rp-C4 HPLC (Higgins Analytical Inc, Proto 300 C4 5μM, 250 x 4.6 mm). Molecular masses of purified analogues were verified using an Applied Biosystems 4700 proteomics analyzer (matrix-assisted laser-desorption/ionization time-of-flight mass spectrometry; MALDI-TOF MS).

[0038] *Circular Dichroism*—Far-ultraviolet (UV) CD spectra were obtained on an AVIV spectropolarimeter equipped with an automated syringe-driven titration unit. Wild type (WT) insulin or insulin analogues were made 50 μM in 10 mM potassium phosphate (pH 7.4) and 50 mM KCl. Spectra were obtained from 190-250 nm. Thermodynamic stabilities were probed by guanidine hydrochloride-induced

denaturation monitored by CD at helix sensitive wavelength 222 nm. Data were fit by non-linear least squares to a two-state-model:

$$\theta(x) = \frac{\theta_A + \theta_B e^{\left(-\Delta G^0_{H_2O} - mx\right)/RT}}{1 + e^{\left(-\Delta G^0_{H_2O} - mx\right)/RT}}$$

where x is the concentration of guanidine hydrochloride, and $\theta_{A,B}$ represent respective estimates of the baseline ellipticities of the protein in its native and unfolded states as extrapolated to a guanidine concentration of 0 M. Baseline values were approximated *via* pre- and post-transition lines represented by equations $\theta_A(x) = \theta_A^{H2O} + m_A x$ and $\theta_B(x) = \theta_B^{H2O} + m_B x$. Such simultaneous fitting avoids artifacts of linear plots of ΔG versus concentration of denaturant.

[0039] *Receptor Binding Assays*—Affinities for IR-A and IR-B were measured by a competitive-displacement scintillation proximity assay. This assay employed solubilized receptor with C-terminal streptavidin binding protein tags purified by sequential wheat-germ agglutinin (WGA) and Streptactin-affinity chromatography from detergent lysates of polyclonal stably transfected 293PEAK cell lines expressing each receptor. A dilution series of recombinant human recombinant insulin (a generous gift from Novo-Nordisk A/S, Bagsværd, Denmark) or analogue (11 dilutions, 5-fold each with a maximum final concentration of 2 µM) in 100 µl binding buffer (100 mM HEPES (pH 7.8), 100 mM NaCl, 10 mM $MgSO_4$, 0.025% (v/v) Tween 20 and 0.5% (w/v) bovine serum albumin) was made in a 96-well plate (Costar). The assay was initiated by addition to the wells of a premixed solution containing WT insulin or insulin analogue in binding buffer supplemented by (i) WGA scintillation-proximity-assay (SPA) beads (Perkin Elmer), (ii) solubilized receptor, and (iii) ^{125}I-Tyr^{A14}-insulin. The final concentration of [^{125}I]-labeled ligand was 7.5 pM, and the amount of receptor added was adjusted so that the extent of labeled ligand binding in the absence of competitor was < 15% of the total added counts in order to avoid ligand-depletion artifacts. Plates were incubated with gentle shaking for 24 h at room temperature, centrifuged, and counted for 5 min/well in a 12-detector Trilux scintillation counter (Perkin Elmer/Wallac). To obtain analogue dissociation constants, competitive binding data were analyzed by non-linear

regression by the method of Wang, a model that provides an analytical solution for the binding of two ligands to a single receptor. A similar method was employed to measure the affinity of a 3-I-Tyr^{B26}-insulin analogue for IGF-1R.

Receptor Binding Screening Protocol—The ability of insulin analogues to displace bound ^{125}I-Tyr^{A14}-insulin from antibody-immobilized WGA-purified receptor was tested at an analogue concentration of 0.75 nM. This concentration corresponded to displacement of 95% of receptor-bound ^{125}I-Tyr^{A14}-insulin by the control analog, Orn^{B29}-insulin. The fraction of ^{125}I-Tyr^{A14}-insulin displaced by a given analogue permitted assignment to the following three categories: (*low affinity*) <60%, (*intermediate affinity*) 61-80% or (*high affinity*) >80%.

[0040] *Assessment of Fibril Formation*—Insulin or insulin analogues were made 60 μM in phosphate-buffered saline (pH 7.4) containing 0.1% sodium azide and gently rocked at 37 °C in glass vials in the presence of a liquid/air interface. Aliquots were taken at regular intervals and frozen for later analysis of thioflavin T (ThT) fluorescence. The assay was terminated on visual appearance of cloudiness.

[0041] *Homology Modeling of μIR Complexes*— Comparative modeling of the 3-I-Tyr^{B26}-insulin variant μIR complex used the MODELLER program. MD simulations adopted as a molecular template the structure of the WT insulin-μIR complex (Protein Data Bank (PDB) entry 4OGA). Several subsets of residues disordered in the crystal structure (IR residues Cys159-Asn168 and Lys265-Gln276 and insulin residues B28-B30) were included as were a single *N*-linked *N*-acetyl glucosamine residue at sites Asn16, Asn25, Asn111, Asn215 and Asn255 as identified in PDB entry 4OGA. An initial set of 50 models was created, and the structure with lowest empirical energy was selected for MD simulations.

[0042] *X-ray Crystallography*—Crystals of 3-I-Tyr^{B26}, Nle^{B29}-insulin were obtained *via* hanging-drop vapor diffusion at 25 °C. 1μl drops containing the protein at 10 mg/ml in 0.02 N HCl were mixed with a 1-μl drop of reservoir buffer containing 0.1 M sodium citrate, 0.08% zinc acetate and 2% phenol. Drops were suspended over 1 ml of reservoir buffer. A single crystal was transferred to a solution containing 30% glycerol in the mother liquor for flash freezing. Diffraction data were obtained using

an in-house X-ray source consisting of a Rigaku rotating-anode X-ray generator (MicroMax^{tm} 007HF with VariMax) with confocal optics, a Saturn 944+ CCD X-ray detector and X-Stream 2000 cryogenic crystal cooling system (located at Case Western Reserve University). Data analysis employed XDS. The structure was determined by molecular replacement using PDB entry 1ZNJ as a starting model, followed by iterative refinement and model building using PHENIX and COOT, respectively. The refinement strategy included both TLS refinement (translation, libration and screw rotation) and torsional non-crystallographic symmetry (NCS) restraints between related chains. Coordinates were deposited under entry code 5EMS with the Protein Data Bank.

[0043] *Molecular Dynamics Simulations*—MD simulations were performed using the GROMACS package of programs (v4.6.1) with OPLS-aa force field. For non-standard residue 3-I-Tyr, a virtual site was placed near the iodine atom to replicate the σ hole. The position of the virtual site was determined by minimizing the error of the fit of the atom-centered charges to the molecular electrostatic potential for 2-iodo-4-methylphenol, calculated at the HF/6-311G(d,p) level. The optimal position of the virtual site was found to be 1.5 Å from the iodine, co-linear with the C-I bond; charges on the virtual site, iodine and carbon attached to iodine were 0.115, -0.322 and 0.207, respectively; charges on all other atoms were adopted from the OPLS-aa parameters for Tyr. Proteins were solvated in a cubic box of TIP4P water molecules; the box extended 10 Å beyond any protein atom. Ionizable residues and protein termini were set in their charged states. Sodium and chloride ions were added to neutralize the system at a final ionic strength of 0.10 M. Protein and solvent (including ions) were coupled separately to a thermal bath at 300 K employing velocity rescaling with coupling time 1.0 ps. Pressure was maintained at 1 bar using a Berendsen barostat with coupling constant 5.0 ps and compressibility 4.5×10^{-5} bar. The time step was 2 fs. Simulations were performed with single non-bonded cutoff 10 Å and neighbor-list update frequency of 10 steps (20 fs). The particle-mesh Ewald method modeled long-range electrostatics; the grid width was 1.2 Å with fourth-order spline interpolation. Bond lengths were constrained using LINCS. The MD protocol consisted of an initial minimization of water molecules, followed by 100 ps of MD

with the protein restrained to permit equilibration of the solvent. Calculations were continued for 200 ns from the geometries obtained after initial positional-restrained MD at a temperature of 300 K.

[0044] *Rodent Assays*—Male Lewis rats (mean body mass ~300 g) were rendered diabetic by treatment with streptozotocin (STZ) as described (Pandyarajan, V., et al. *J. Biol. Chem.* **289**, 34709-27 (2104)). To test the *in vivo* potency of insulin analogues in relation to Orn^{B29}-insulin or Nle^{B29}-insulin, protein solutions containing insulin analogues were constituted in a buffer composed of 16 mg glycerin, 1.6 mg *meta*-cresol, 0.65 mg phenol and 3.8 mg sodium phosphate (pH 7.4). Insulin analogues were injected intravenously (IV) into tail veins at a dose of 10 µg per 100 µl of buffer per 300 g rat. The resulting changes in blood-glucose concentration were monitored by serial measurements using a clinical glucometer (EasyMax Voice Blood Glucose Meter) over the next several hours. Insulin analogues were each re-purified by reverse-phase HPLC, dried to powder, dissolved in diluent at the same maximum protein concentration and re-quantitated by analytical C4 reverse-phase HPLC; dilutions were made using the above buffer.

[0045] Rats were injected IV at time $t = 0$. Blood was obtained from the clipped tip of the tail at time $t = 0$ and every 10 min for the first hour, every 20 min for the second hour, every 30 min for the third hour and every hour thereafter up to 360 min. Although studies of the high-affinity natural analogues were limited in size (N = 5 rats), the impact of the iodo-Tyr^{B26} modification was evaluated with greater power. Studies of the 3-I-Tyr^{B26}-Nle^{B29}-insulin were thus repeated (in relation to Nle^{B29}-insulin) on four dates over six months to avoid confounding variables that may impact the environment of the rat colony week to week. Rats studied on each date (N = 4 or 5) were obtained at random from a large colony (50 rats). Levels of mean glycemia at baseline were similar in each group and at each date; similar individual trends were observed at each date. The efficacy of insulin action in reducing blood-glucose concentration was calculated using (a) the change in concentration over the first hour (d[glucose]/dt); (b) the integrated area between the glucose time dependence and a near-horizontal line from the starting blood glucose concentration to the final concentration; and (c) the integrated area for the same curve in the first 0-80 min

versus that observed in the 80-360 min interval (the latter representing the delayed "tail" of insulin action). Areas under the linear upper hyperglycemic baseline and above the curve representing observed blood-glucose concentrations were estimated by trapezoidal approximation and denoted AOC. Assessment of statistical significance was performed using Student's *t*-test.

EXAMPLE

[0046] *Receptor-binding studies define three classes of analogs*. To obtain an initial overview of how substitutions at position B26 affect the properties of insulin, 19 insulin analogues containing substitutions at B26 were prepared at small scale (Table 1). To eliminate the B29 tryptic site (and so facilitate semi-synthesis; 58), these initial analogues each contained Orn^{B29} (in place of Lys^{B29}). Similarly, to provide a basic side chain at B26, an analogue was prepared containing both substitutions Orn^{B26} and Orn^{B29}. Cys^{B26}-Orn^{B29}-insulin was not prepared to avoid possible disulfide interchange and/or formation of covalent dimers.

[0047] A coarse receptor-binding assay (using IR-B) was first undertaken, which enabled subgroups of the insulin analogues to be distinguished based on displacement of pre-bound ^{125}I-labeled insulin at a uniform analogue concentration of 0.75 nM (Fig. 3*A*). At this concentration WT insulin displaced 90% of the prebound tracer (^{125}I-Tyr^{A14}-insulin; see Experimental Procedures). The results defined three classes (Fig. 3*B*): (i) high affinity (tracer displacement >80%; *i.e.*, similar or greater than that observed on binding of WT insulin); (ii) intermediate affinity (tracer displacement 61-79%) and (iii) low affinity (tracer displacement <60%). The low-affinity class contained two aliphatic residues (Ile and Leu). The intermediate-affinity class comprised a diverse set of residues, including Phe, Met, Pro, Thr and Val; the remaining analogues (representing 10 of the 19 analogues tested) were placed in the high-affinity group.

[0048] Definitive IR-B binding assays were then undertaken of selected high-, intermediate- and low-affinity analogues (Table 1) using a scintillation proximity assay performed with purified detergent-solubilized receptor isoform expressed in the same cell line. Affinities greater than WT insulin were conferred only by Ser^{B26} and

Glu^{B26} (K_d ~ 0.02 nM) whereas the affinities conferred by Tyr^{B26}, Ala^{B26} and Orn^{B26} were indistinguishable (K_d ~ 0.04 nM). The high affinities of Ala^{B26} and Glu^{B26} insulin analogues have previously been reported. Also in accordance with data known in the art, substitution of Tyr^{B26} by Phe reduced affinity (between two- and threefold). Whereas a similar reduction was conferred by Val^{B26}, substitution of Tyr^{B26} by Ile or Leu led to more severe impairments (by ~10-fold and 30-fold, respectively).

[0049] For four analogues of high IR-B binding affinity (Ala, Asn, Glu and Ser), comparative IR-A versus IR-B binding assays were performed relative to WT insulin. In particular, the affinity of Asn^{B26}-insulin for either receptor isoform was similar to that of WT insulin (Fig. 4). Although in these assays Asn^{B26}-Orn^{B29}-insulin (*triangles* in Fig. 4) exhibited a trend toward a slight decrease in affinity (*ca.* 10%) relative to Orn^{B29}-insulin (*squares*), such small differences did not achieve statistical significance as standard errors of the mean were in the range 10-20% relative to mean values. The absence of isoform selectivity is in accordance with our design goals.

[0050] Two sets of observations were particularly striking: (a) the high affinity of analogues containing charged side chains (of either sign) or a short polar side chain (Ser) at B26 and (b) the functional incompatibility of aliphatic substitutions larger than Ala at B26.

[0051] *CD studies of high-affinity analogues provide evidence of native-like structure with decreased dimerization*. Although well tolerated in relation to receptor binding, substitution of Tyr^{B26} by Orn, Glu or Ser was in each case associated with an altered far-UV CD spectrum at a protein concentration of 50 μM (Fig. 5*A*). At this concentration WT insulin, and presumably also Orn^{B29}-insulin, is predominantly dimeric as is well known in the art. The variant spectra exhibited attenuated ellipticity at 222 nm and deepening of the minimum near 208 nm, spectroscopic features associated with partial loss or dynamic destabilization of α-helices. Although not wishing to be bound by theory, we ascribe these CD changes to decreased dimerization. It is possible that polar or charged substitutions of Tyr^{B26} could also impair the segmental stability of the neighboring A1-A8 α-helix as the native side

chain adjoins the β-branched side chains of Ile^{A2} and Val^{A3} within an inter-chain crevice.

[0052] *Functional substitutions impair thermodynamic stability.* Substitutions Orn^{B26}, Glu^{B26} and Ser^{B26} impaired global stability. Estimates of respective free energies of unfolding (ΔG_u) were obtained at 25 °C based on CD studies of fractional unfolding on chemical denaturation (Fig. 5*B* and histogram in Fig. 5*G*). A trend was observed wherein lower concentrations of denaturant (guanidine hydrochloride) were required for 50% unfolding of analogues containing the above substitutions (Fig. 5*B* and Table 2, column 3). Application of a two-state model (native and unfolded) yielded ΔG_u values that were in each case at least 0.5 kcal mol^{-1} lower than that of Orn^{B29}-insulin (baseline stability 3.2(±0.1) kcal mol^{-1}). Respective decrements in stability ($\Delta\Delta G_u$) for the Orn^{B26}, Glu^{B26} and Ser^{B26} analogues were 0.7(±0.2), 0.9(±0.2) and 0.9(±0.2) kcal mol^{-1}. Such perturbations were thus similar to that reported in studies of an insulin analogue containing substitution of Phe^{B24} by Ala ($\Delta\Delta G_u$ 0.8(±0.2) kcal mol^{-1}).

[0053] The *m*-values obtained in the fitting (which correlate with extent of solvation of nonpolar surfaces on protein denaturation) were significantly attenuated relative to Orn^{B29}-insulin or WT insulin (column 4 in Table 2). Such attenuation suggests that, in their respective natives states, the analogues exhibit less efficient desolvation of nonpolar surfaces. This trend may be due a direct perturbation of the (A2, A3)-related inter-chain crevice by Orn^{B26}, Glu^{B26} and Ser^{B26}; transmitted structural perturbations cannot be excluded.

[0054] *Functional substitutions lead to accelerated fibrillation.* The reduced stabilities and *m*-values of the Orn^{B26}, Glu^{B26} and Ser^{B26} analogues motivated assessment of lag times prior to onset of fibrillation relative to Orn^{B29}-insulin (Fig. 5*H* and column 5 in Table 2). Although Orn^{B29}-insulin exhibited a broad range of lag times greater than 5 days (with a mean of 13 days in N = 14 trials), the analogues consistently exhibited lag times less than 4 days (N = 3). Despite the small sample size, *p*-values were 0.06 (Glu^{B26}) or < 0.05 (Orn^{B26} and Ser^{B26}). These trends are therefore unrelated to the charge of the B26 side chain and net charge of the protein.

While not wishing to be bound by theory, we speculate that perturbation of the (A2, A3)-related inter-chain crevice favors local unfolding and non-native conformational excursions, in turn favoring formation of an amyloidogenic nucleus. These findings suggest that, of the naturally occurring amino acids, Tyrosine has been conserved at position B26 because it confers the best combination of activity and stability. The decreased physical stability of the high-affinity subclass of variants at this site further suggest that insulin analogues containing natural amino-acid substitutions at position B26 would not be suitable for clinical use in a pharmaceutical formulation.

[0055] *A non-standard B26 modification augments receptor binding while preserving stability.* Semi-synthesis enabled efficient preparation of 3-I-Tyr^{B26}-substituted Orn^{B29}-insulin; a related 3-I-Tyr^{B26}-substituted analogue containing trypsin-insensitive norleucine^{B29} (Nle) was also prepared in the course of crystallization trials (below). The affinities of these analogues for IR-B (Table 1) were enhanced two to three fold (relative to respective parents Orn^{B29}-insulin and Nle^{B29}-insulin) in accordance with past studies of 3-I-Tyr^{B26}-substituted WT insulin. The iodinated analogue also exhibited a three-to-four fold increase in affinity for IGF-1R.

The 3-I-Tyr^{B26} modification was found to preserve native-like structure, stability and resistance to fibrillation. In particular, (i) CD spectra of Orn^{B29}- and Nle^{B29}-insulin and their respective 3-I-Tyr^{B26}-substituted derivatives were similar in the absence of zinc ions (Fig. 5*C-F*), suggesting that the iodo-aromatic modification preserves native secondary structure. (ii) CD-detected studies of chemical protein denaturation likewise indicated similar thermodynamic stabilities (Table 2). (iii) No significant differences were observed between the fibrillation lag times of 3-I-Tyr^{B26} analogues and their respective parents (Fig. 5*H*). Maintenance of resistance to fibrillation stands in contrast to the foreshortened lag times associated with functional non-aromatic side chains at B26 (Glu^{B26}, Ser^{B26} and Orn^{B26}; see above). Studies of 3-I-Tyr^{B26} in combination with Orn^{B26} did not reveal significant foreshortening of the duration of insulin action in the diabetic rats.

[0056] *Crystal structure of 3-I-Tyr^{B26}-Nle^{B29}-insulin demonstrates insertion of the iodine atom within a nonpolar crevice.* The analogue was crystallized under conditions that ordinarily lead to crystallization of WT insulin as a phenol-stabilized

R_6 hexamer. A monoclinic lattice was observed in which one R_6 hexamer defined the asymmetric unit (Table 3). In this crystal form each insulin protomer in the hexamer is crystallographically independent (and so may in principle exhibit subtle structural differences). A ribbon model of this hexamer (Fig. 6*A*) highlights the positions of the iodine atoms (*large gray* spheres) relative to the six R-state-specific B1-B19 α-helices (*medium gray*) and A chains (*black*).

[0057] No significant differences were observed between the modified hexamer and the corresponding WT R_6 hexamer with respect to secondary structure, chain orientation, mode of assembly, or structures of the Zn^{2+}- and phenol binding sites. The six independent R-state protomers exhibited essentially identical conformations [average pairwise main-chain root-mean-square difference (rmsd) = 0.42 Å and average side-chain rmsd = 1.43 Å]. Tetrahedral coordination of the two axial zinc ions (overlying *small* spheres at center in Fig. 6*A*) by the side chains of His^{B10} (three per R_3 trimer; *light gray* side chains) is essentially identical to that in WT R_6 hexamers; the fourth coordination site in each case contains a presumed chloride anion.

[0058] Superposition of a representative analogue protomer and WT protomer (*dark* and *light gray* ribbons respectively in Fig. 6*B*) yielded the following average pairwise differences between a representative protomer of 3-I-Tyr^{B26}-Nle^{B29}-insulin and the WT R-state: main-chain rmsd 0.55(±0.08) Å and side-chain rmsd 1.94(±0.23) Å. These values are similar to those observed among a collection of independent WT R-state protomers (main-chain rmsd 0.68(±0.26) Å; side-chain rmsd 1.14 (±0.34) Å). Within the crystal structure of 3-I-Tyr^{B26}-Nle^{B29}-insulin, no polypeptide-like ($2F_{obs}$-F_{calc}) electron density (continuous at >1σ) was observed C-terminal to the respective Pro^{B28} residues within chains B, D, H, J and L; in the case of chain F, continuous density beyond Pro^{B28} was observed at the >0.5σ level, but could not be reasonably modeled as a single conformation.

[0059] The overall similarity of the variant and WT structures suggests that the essential features required for dimer formation are not altered by the asymmetric distribution of partial charges in the aromatic ring of Tyr^{B26} and its associated pattern of aromatic-aromatic interactions (Fig. 6*C*). The six independent side chains of 3-

iodo-Tyr^{B26} nonetheless exhibit similar conformations, each distinct from that of the WT Tyr^{B26} (Fig. 6*D*). The modified side chain (*dark gray* in Fig. 6*D*) is rotated by ~12° about the C_α-C_β bond with respect to its counterpart in the WT (*light gray* in Fig. 6*D*). This rotation positions the iodo-group within a non-polar pocket formed by the side chains of residues Ile^{A2}, Val^{A3}, Leu^{B11} and Val^{B12}—these residues are each conserved among vertebrate insulins and essential for biological activity as well known in the art. In the WT structure the pocket is occupied by the phenolic hydroxyl group of Tyr^{B26}, although its packing within the pocket is less intimate than that exhibited by the iodo-group in the analog. The displacement of the *para*-hydroxyl group of 3-I-Tyr^{B26} from the pocket results in its greater solvent exposure. Side-chain dihedral angles of three aromatic side chains at or near the dimer interface (B16, B24 and B26) are given in Table 4 in relation to a reference WT R_6 structure.

[0060] The analogue hexamer contains six bound molecules of phenol, located at an interface between dimers as in the WT R_6 hexamer. The six independent phenol-binding sites are essentially identical. The ($2F_{obs}$ - F_{calc}) electron-density map volume associated with one such phenol is shown in relation to a superposition of variant and WT structures (*dark* and *light gray* in Fig. 7*A-B*; stereo stick models). In each case a characteristic pair of hydrogen bonds from the phenolic –OH group is formed to the main-chain carbonyl oxygen (acceptor) and amide group (donor) of Cys^{A6} and Cys^{A11}, respectively. An expanded view of the corresponding B26 side chain environment is shown in (Fig. 7*C-D*).

[0061] The re-arrangement of the iodo-substituted B26 side chain does not alter the canonical hydrogen-bonding pattern of the anti-parallel β-strand formed by the juxtaposed B24-B26 segments within the analogue dimer (Fig. 8*A*). A disparity with respect to the WT is observed, however, at Phe^{B25}. In the WT structure (PDB 1ZNJ) the side chain of this residue shows one of two populated χ_1 angles ($\chi_1 \approx 45°$ or $\chi_1 \approx -106°$) but similar χ_2 angles ($\chi_2 \approx -82)°$, with either full or partial occupancy (Fig. 8*B*). In contrast, within each dimer pair within the analogue hexamer, the side chains of the respective two Phe^{B25} residues exhibit a more limited range of χ_1 angle variation (χ_1 = -136°, 165°; χ_1 = -163°, -160°; χ_1 = -168°, -145°) than in the WT structure, but wider

range of χ_2 angles (χ_2 = 60°, 72°; χ_2 = 75°, -7°; χ_2 = 8°, -87°; see Fig 7B). We note, however, that for residue 25 in three B-chains (*viz.* chains B, D and H) (i) the side-chain conformations that best fit the density do not in general correspond to standard side-chain rotameric conformations and (ii) the side-chain density is poor, suggesting dynamic disorder. We speculate that these differences in side-chain conformation at Phe^{B25} may arise from slight alterations in backbone geometry resulting from accommodation of the iodine atom at B26. Subtle variation in the crystallization milieu cannot be excluded.

[0062] The environment (and the conformation) of iodo-Tyr^{B26} in the variant hormone-IR complex is likely to differ from the internal and non-polar environment in the modified zinc hexamer, given that in the co-crystal structure of the WT μIR complex, the B23-B27 segment is displaced from its location in the free hormone. Such displacement permits the three aromatic rings of Phe^{B24}, Phe^{B25} and Tyr^{B26} to contact the ectodomain. The receptor-bound conformation of the hormone is thus predicted to expose the side chain of 3-I-Tyr^{B26} and in particular enable its modified ring to engage the L1 surface. An MD-based model of such a variant complex is presented in the Discussion in relation to possible halogen bonding as a mechanism to augment IR binding. We therefore envisage that, on receptor engagement, the iodine atom swaps between internal- (non-polar) and external (polar) interfaces.

[0063] *Rat studies of selected insulin analogs.* The glucose- lowering activity of representative analogues with high IR-binding affinities were tested by IV bolus injection of a submaximal dose into rats rendered diabetic by STZ.[7] Data are shown in relation to the absolute blood-glucose concentration (left-hand panels in Fig. 9) and relative to the initial level of glycemia (right-hand panels). The Orn^{B29}-insulin template was indistinguishable from WT insulin and insulin *lispro* (an insulin analogue in clinical use) in potency and duration of action (Fig. 9*A*, *B*). Each of the analogues containing B26 substitutions exhibited biological activity. In these studies Glu^{B26}-Orn^{B29}-insulin was indistinguishable from Orn^{B29}-insulin (respective *light gray* and *medium gray* filled circles in Fig. 9*C*, *D*); a trend toward lower activity was exhibited by Ser^{B26}-Orn^{B29}-insulin despite its enhanced IR affinity (*dark gray*). The statistical significance of these differences was limited by the sample size (N = 5; see

also caption to Fig. 9). Orn^{B26}-Orn^{B29}-insulin exhibited a similar trend relative to Orn^{B29}-insulin (*light gray* and *dark gray* circles, respectively, in Fig. 9*E*, *F*).

[0064] *Rat studies of 3-I-Tyr^{B26}-Nle^{B29}-insulin suggest favorable pharmacodynamics properties*. In the Nle^{B29} template the 3-I-Tyr^{B26} modification leads to a similar initial rate of decline in blood-glucose concentration but a more rapid recovery between 80-360 min (Fig. 10*A*, *B*). These studies represent the average of 18 animals receiving Nle^{B29}-insulin and 20 animals receiving 3-I-Tyr^{B26}-Nle^{B29}-insulin. Glycemic responses were first analyzed with respect to initial rate of fall in blood-glucose concentration (t = 0-60 min). Results of individual rats are shown as dot-box plots (Fig. 10*C*) and summarized in histograms (Fig. 10*D*) relative to WT insulin (N = 5). Respective initial rates of fall were indistinguishable.

[0065] Visual inspection of the primary data (Fig. 10*A*, *B*), suggested that 3-I-Tyr^{B26}-Nle^{B29}-insulin was associated with a more rapid recovery of hyperglycemia at later times (80-360 min). To obtain an integrated measure of insulin action in each animal, the area bounded by the upper line connecting the initial and final [glucose] values and the observed lower [glucose] values (connected by line segments) was measured at intermediate and later times. These integrated measures are indistinguishable during the first 80 min (Fig. 9*E*). Significantly, for the 3-I-Tyr^{B26} analogue the delayed tail of insulin action (80-360 min) was attenuated relative to the parent analogue ($p < 0.05$, Fig. 10*F*). This trend was also observed on IV injection of twice the dose (data not shown). Such foreshortening of signaling may be of therapeutic advantage for patients using an insulin pump due to the risk of hypoglycemia associated with a prolonged tail.

Table 1. Receptor-Binding Affinities of Insulin Analogs[a]

B26 residue	K_d (nM)	B24 residue	K_d (nM)
Tyr[b]	0.042 ± 0.007	Pro	I[d]
Gly	H[c]	Ser	0.021 ± 0.003
Ala	0.042 ± 0.007	Thr	I
Val	0.12 ± 0.02	Cys	ND[e]
Leu	1.2 ± 0.2	Asn	H
Ile	0.52 ± 0.08	Asp	H
Met	I	Gln	0.043 ± 0.007
3-I-Tyr[f]	0.022 ± 0.004	Glu	0.021 ± 0.002
Phe	0.10 ± 0.020	His	H
Trp	H	Orn[g]	0.038 ± 0.006

[a]Analogues were prepared in a template in which Lys^{B29} was substituted by Orn unless otherwise noted. Assays employed the B isoform of the purified and detergent-solubilized IR as described.

[b]This represents Orn^{B29}-insulin; the dissociation constant of WT insulin under these conditions was 0.042 nM.

[c]H represents the high-affinity group in the initial coarse screening (Fig. 3B).

[d]I represents the intermediate-affinity group in the initial coarse screening (Fig. 3B).

[e]ND; not determined as the Cys^{B26} analogue was not prepared.

[f]Corresponding K_d in the context of Nle^{B29} was 0.021 ± 0.005 nM versus 0.062 ± 0.008 nM (Nle^{B29}-insulin parent).

[g]Orn^{B26} provided a model of a basic side chain as Lys or Arg would have complicated semi-synthesis (see Experimental Procedures).

Table 2. Properties of Insulin Analogues

Protein	ΔG_u[a] (kcal mol^{-1})	C_{mid} (M)	*m* (kcal mol^{-1} M^{-1})	fibril. lag time[b] (days (N))
wild-type insulin	3.4 ± 0.1	4.8 ± 0.1	0.69 ± 0.02	2.3 ± 1.1
Orn^{B29}-insulin	3.2 ± 0.1	4.8 ± 0.1	0.66 ± 0.01	13.1 ± 6.5
Glu^{B26}-Orn^{B29}	2.3 ± 0.1	4.4 ± 0.1	0.53 ± 0.02	2.7 ± 0.6
Orn^{B26}-Orn^{B29}	2.5 ± 0.1	4.3 ± 0.2	0.59 ± 0.03	2.0 ± 0.5[c]
Ser^{B26}-Orn^{B29}	2.3 ± 0.1	4.3 ± 0.3	0.53 ± 0.04	2.0 ± 0.5[c]
3-I-Tyr^{B26}-Orn^{B29}	3.2 ± 0.1	4.9 ± 0.2	0.65 ± 0.02	12 ± 1.7
Nle^{B29}	3.4 ± 0.1	4.8 ± 0.1	0.71 ± 0.01	14.3 ± 1.6
3-I-Tyr^{B26}-Nle^{B29}	3.4 ± 0.1	4.9 ± 0.1	0.69 ± 0.02	14.3 ± 1.5

[a]Thermodynamic parameters were inferred from CD-detected guanidine denaturation data by application of a two-state model.

[b]Fibrillation lag times pertain to zinc-free wild-type insulin (in a monomer-dimer equilibrium) and analogues (monomeric); each protein was made 60 μM in phosphate-buffered saline (pH 7.4). A twofold increase over baseline in ThT fluorescence provided a criterion for onset of fibrillation.

[c]All individual samples in this set exhibited the same lag time of 2 days. As the method employed in this study could not distinguish fibril lag times with a resolution given in hours, some variance was added to the data by adding ± 0.1 to individual data points in order to obtain standard deviations.

Table 3. X-ray Data Processing and Refinement Statistics

Data Processing	
Wavelength (Å)	1.5478
Resolution range (Å)	40.85 - 2.30 (2.40 - 2.30)[a]
Space group	$P2_1$
a (Å), *b* (Å), *c* (Å), β (°)	46.43, 61.63, 58.58, 111.38
Redundancy	4.76 (2.55)
Completeness (%)	95.6 (80.4)
R_{merge}	0.054 (0.227)
$< I/\sigma(I) >$	18.2 (3.9)
$CC_{1/2}$ [b]	0.999 (0.934)
Refinement	
Resolution range (Å)	40.85 - 2.30
No. reflections	13255
R_{work} / R_{free} [c]	0.163 / 0.228
No. protein atoms	2305
No. non-protein atoms	121
$< B_{iso} >$ protein atoms (Å^2)	41.6
$< B_{iso} >$ non-protein atoms (Å^2)	34.0
σ_{bonds} (Å) / σ_{angles} (°)	0.008/1.12
Ramachandran plot	
Favored (%)	100
Outliers (%)	0

[a]Numbers in parentheses refer to the outer resolution shell.

[b]Pearson correlation coefficient between merged intensities of two random halves of the diffraction data set.

[c]Free set contained 10% of total observed reflections.

Table 4. Side-chain dihedral angles of aromatic side chains near dimer interface[a]

	Iodo-Tyr^{B26} analog		WT[b]	
Residue	χ_1 (°)	χ_2 (°)	χ_1 (°)	χ_2 (°)
Tyr^{B16}	172.4	78.8	174.7	77.6
	176.9	83.1	179.6	80.8
	175.4	82.9	172.9	84.3
	174.5	81.1	177.6	84.6
	177.0	79.2	175.9	75.5
	178.0	79.6	175.3	66.2
Phe^{B24}	63.2	-87.6	62.5	89.1
	69.9	88.42	69.3	83.2
	60.0	-85.33	59.3	83.4
	63.0	-86.9	55.2	-85.0
	60.1	-89.0	56.7	-87.9
	61.0	-87.5	68.8	87.5
Tyr^{B26}	167.8	74.1	-173.9	82.7
	166.6	81.0	168.9	-90.5
	161.4	72.6	-176.7	69.8
	167.7	75.3	176.5	74.7
	168.1	75.7	-173.9	80.1
	165.3	78.0	175.4	72.4

[a]Phe^{B25} has been excluded due to poor side-chain density found in the crystal structure

[b]PDB entry: 1ZNJ

CLAIMS

What is claimed is:

1. An insulin analogue comprising an insulin B-chain polypeptide sequence containing a 3-iodo-Tyrosine or (3,5)-di-iodo-Tyrosine at position B26 relative to the positions of a wild type insulin B chain.

2. The insulin analogue of claim 1, additionally comprising a substitution at a position corresponding to position B29 relative to the positions of a wild type insulin B chain, selected from a standard or non-standard amino-acid residue containing a neutral or acidic side chain.

3. The insulin analogue of claim 2, comprising SEQ. ID 4.

4. The insulin analogue of claim 2, wherein residue B29 is Glutamic Acid or Aspartic Acid.

5. The insulin analogue of claim 2, wherein residue B29 is Alanine, Leucine, Isoleucine or Valine.

6. The insulin analogue of claim 2, wherein residue B29 is amino-proprionic acid, amino-butyric acid, or norleucine.

7. The insulin analogue of claim 6, comprising SEQ ID NO: 5.

8. The insulin analogue of any one of claims 1-7, wherein the insulin analogue is a two-chain insulin analogue.

9. The insulin analogue of any one of claims 1-7, wherein the insulin analogue is a single-chain insulin analogue.

10. A nucleic acid sequence encoding the insulin analogue of any one of claims 1-7, wherein the iodo-modified or di-iodo-modified Tyrosine residue is encoded by a stop codon.

11. An expression vector comprising the nucleic acid sequence of claim 10.

12. A host cell transformed with the expression vector of claim 11.

13. A method of lowering the blood sugar of a patient in need thereof, the method comprising administering a physiologically effective amount of an insulin analogue or a physiologically acceptable salt thereof to the patient, wherein the insulin analogue is an insulin analogue of claim 8.

14. The insulin analogue of claim 8, for use as a medicament.

15. The use of the insulin analogue of claim 8 for the manufacture of a medicament for the treating of diabetes mellitus.

16. The insulin analogue of claim 8, for the treatment of diabetes mellitus.

17. A method of lowering the blood sugar of a patient in need thereof, the method comprising administering a physiologically effective amount of an insulin analogue or a physiologically acceptable salt thereof to the patient, wherein the insulin analogue is an insulin analogue of claim 9.

18. The insulin analogue of claim 9, for use as a medicament.

19. The use of the insulin analogue of claim 9 for the manufacture of a medicament for the treating of diabetes mellitus.

20. The insulin analogue of claim 8, for the treatment of diabetes mellitus.

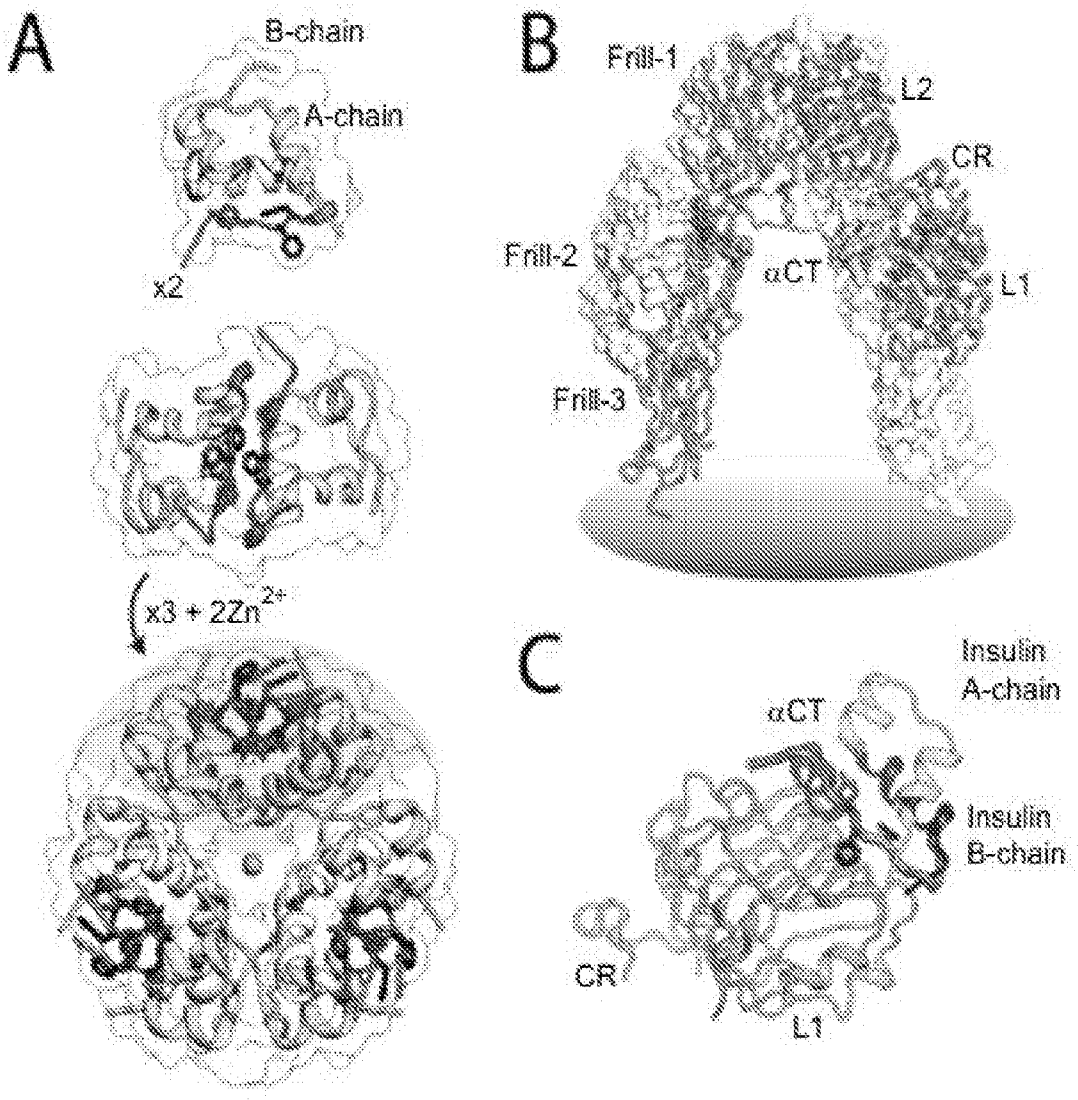

FIG. 1
(prior art)

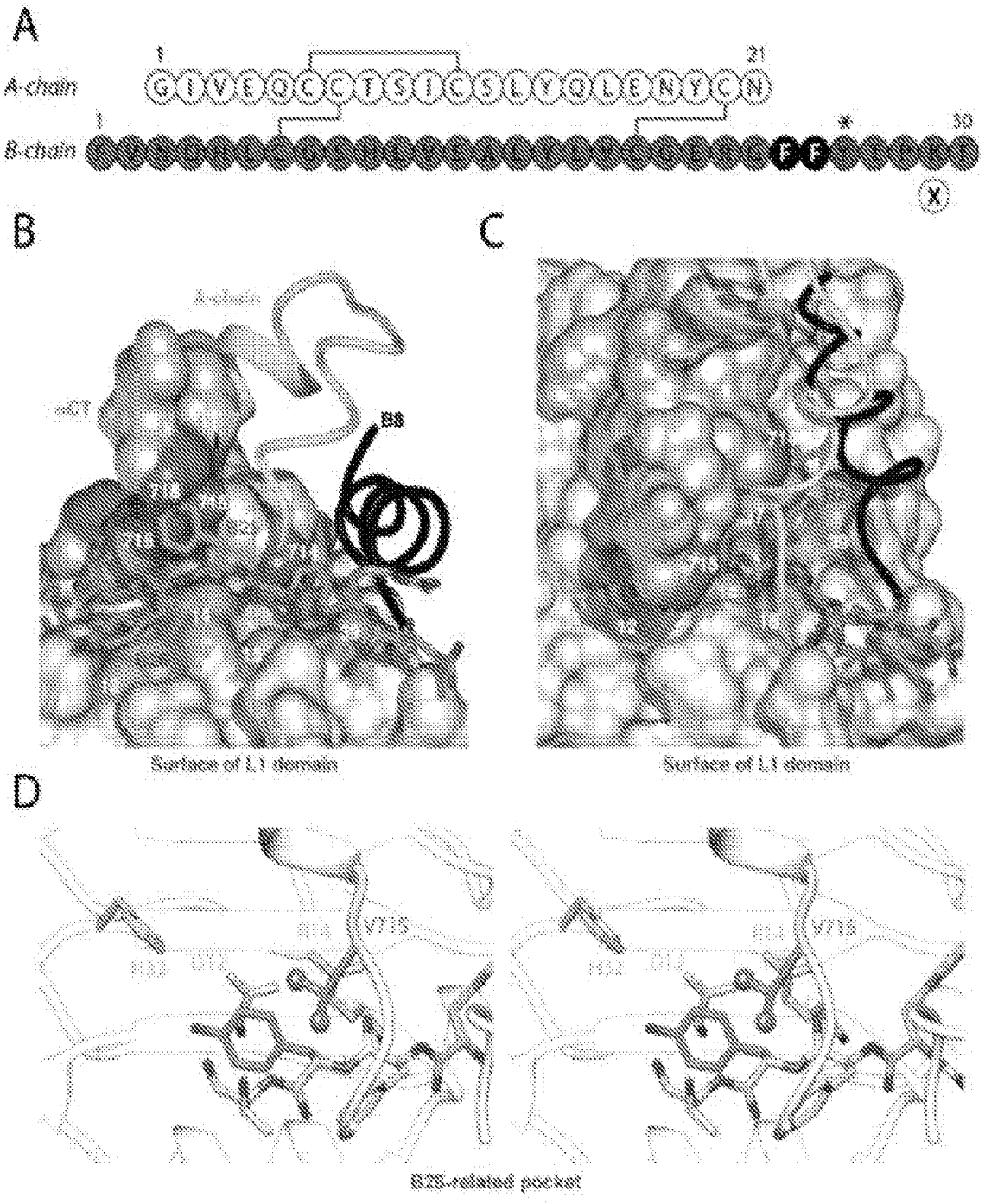

FIG. 2
(prior art)

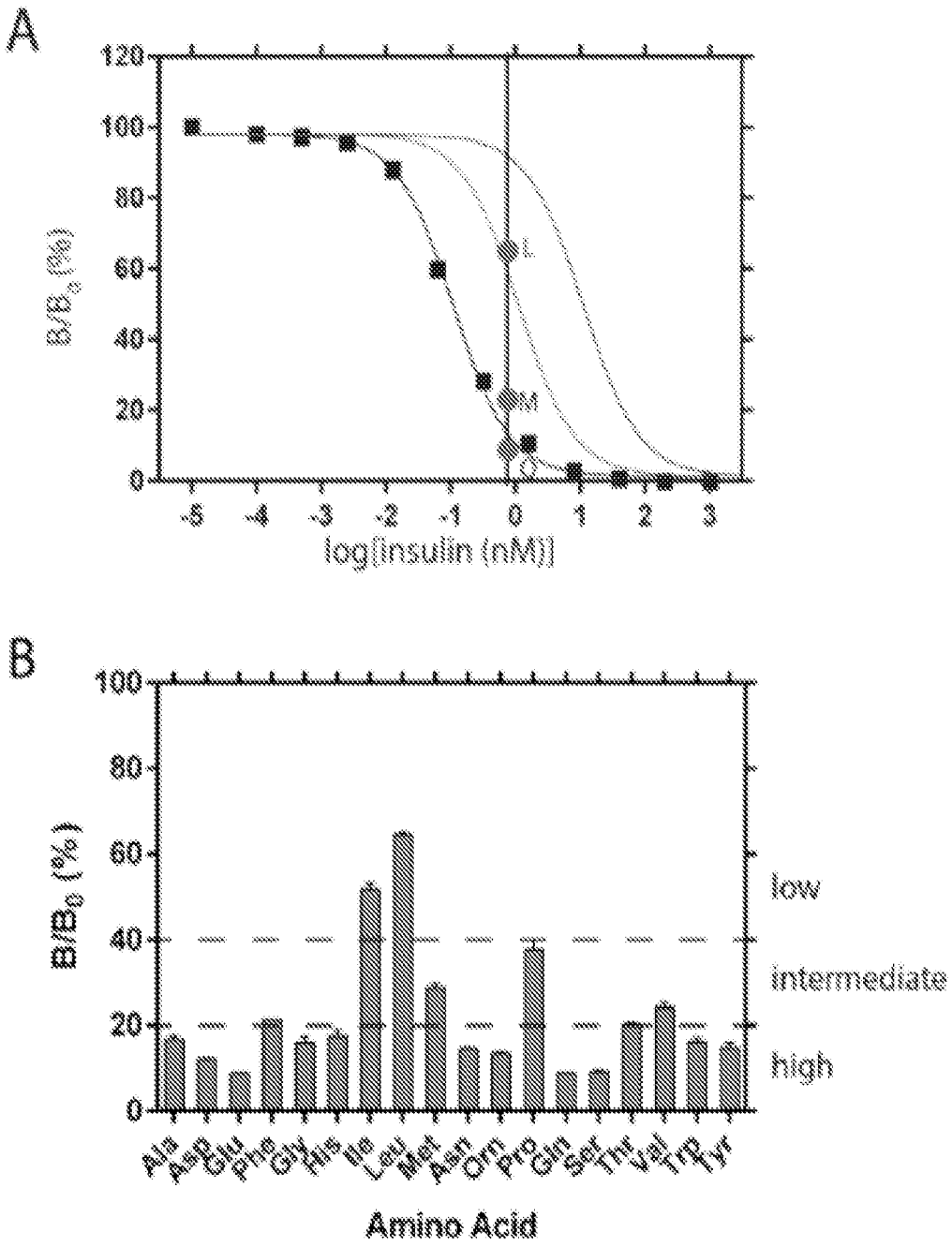
A
120
100
80
60
40
20
0
B/B0 (%)
L
M
O
-5
-4
-3
-2
-1
0
1
2
3
log [insulin (nM)]
B
100
80
60
40
20
0
B/B0 (%)
low
intermediate
high
Ala
Asp
Glu
Phe
Gly
His
Ile
Leu
Met
Asn
Orn
Pro
Gln
Ser
Thr
Val
Trp
Tyr
Amino Acid

FIG. 3

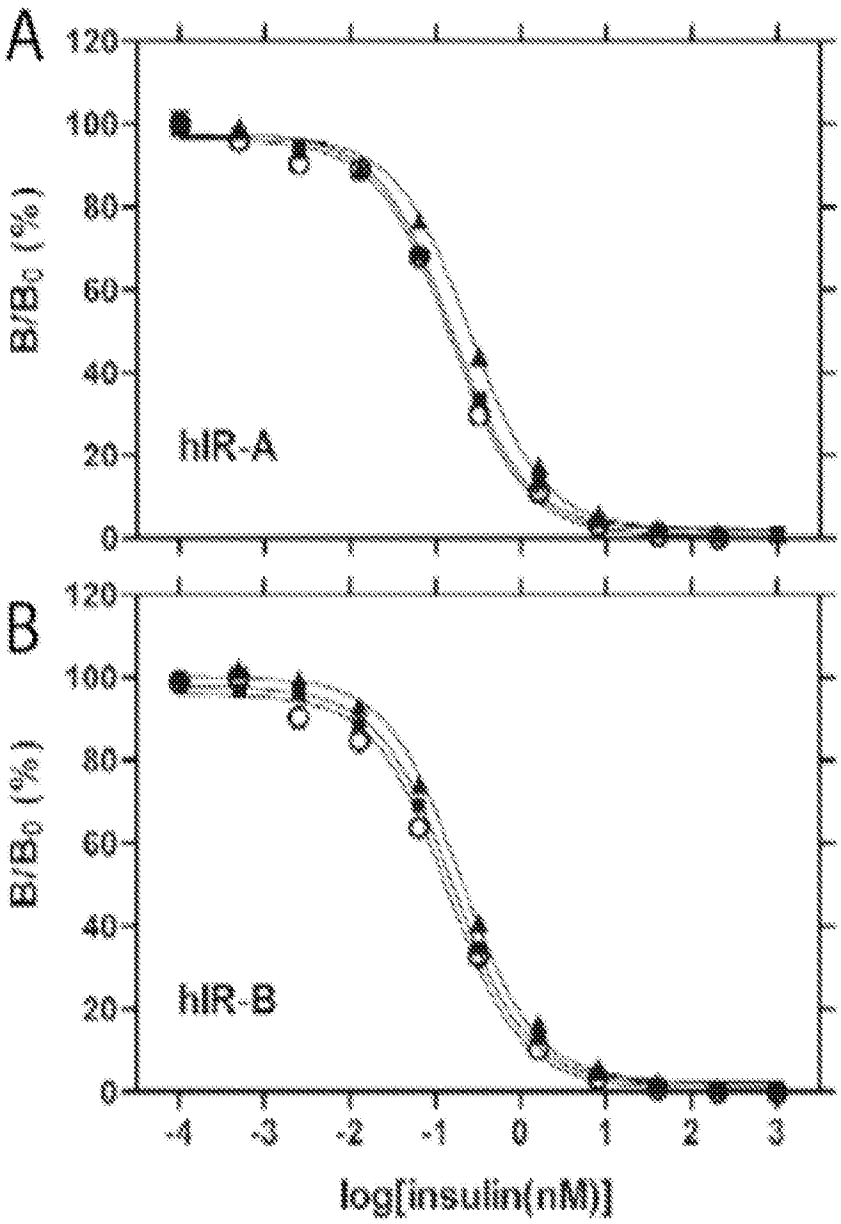

FIG. 4

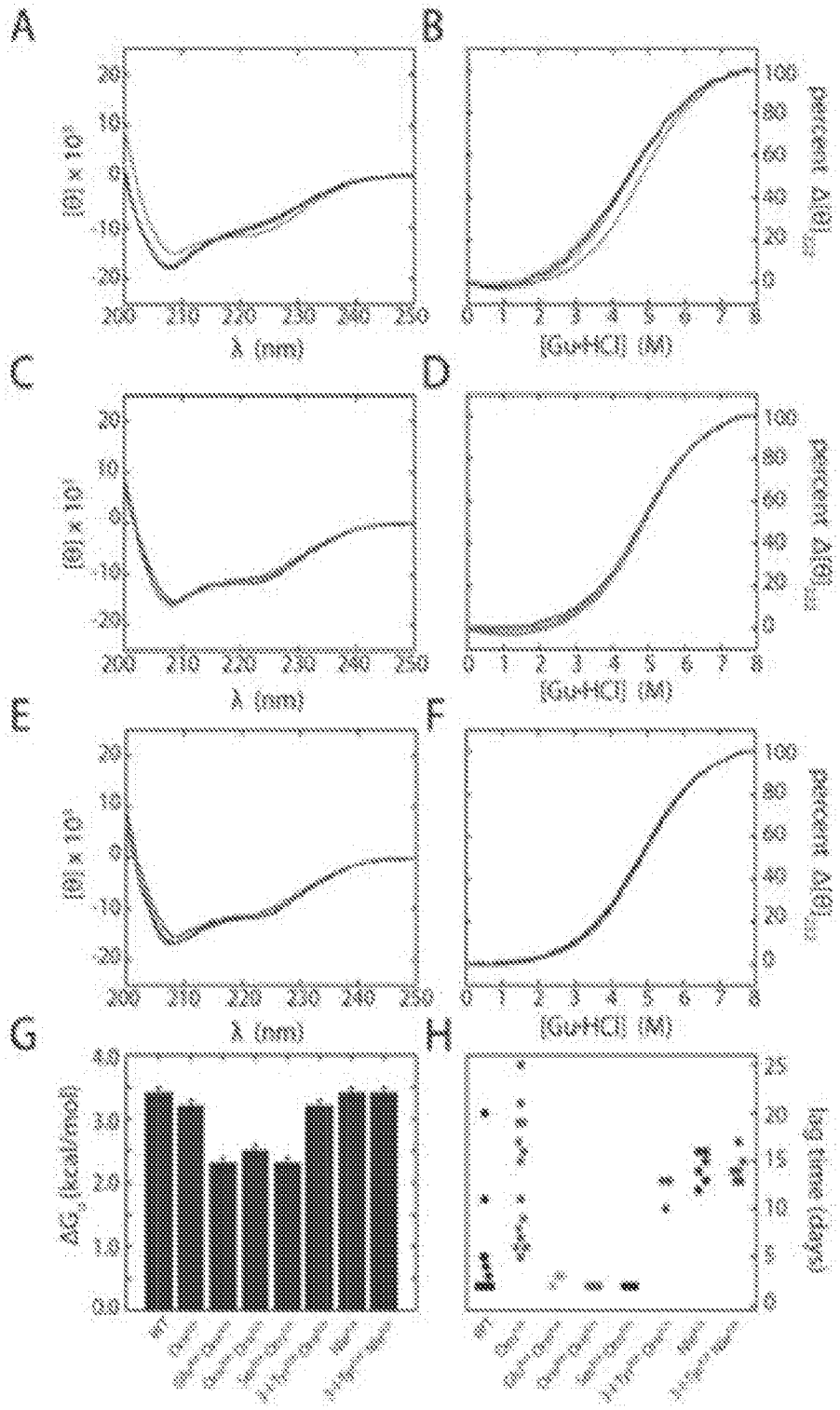

FIG. 5

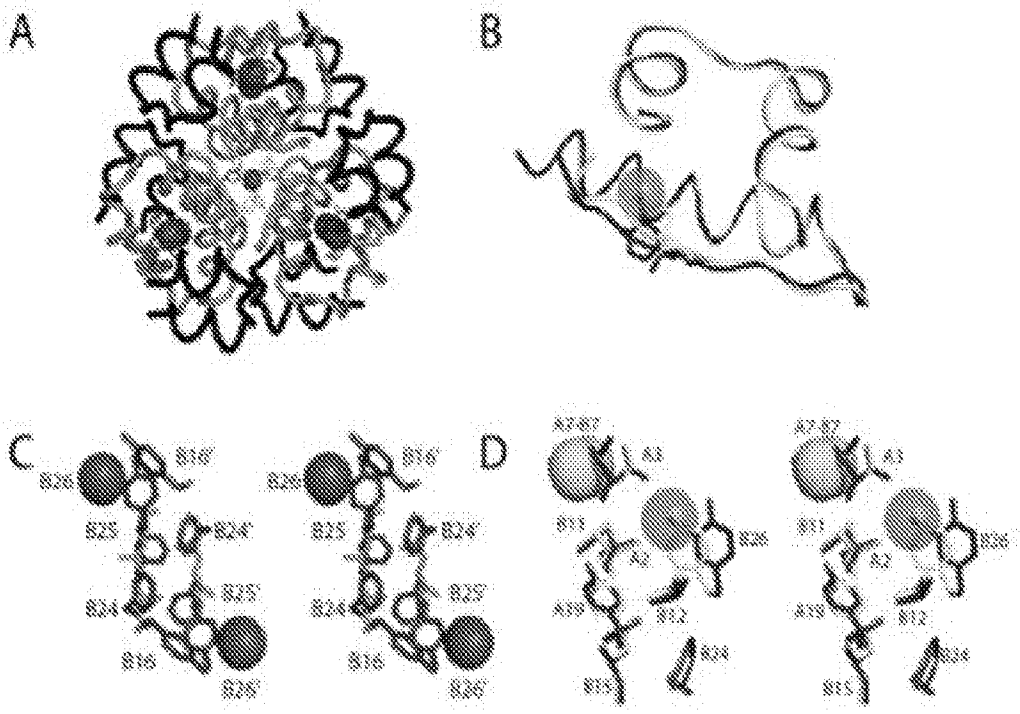

FIG. 6

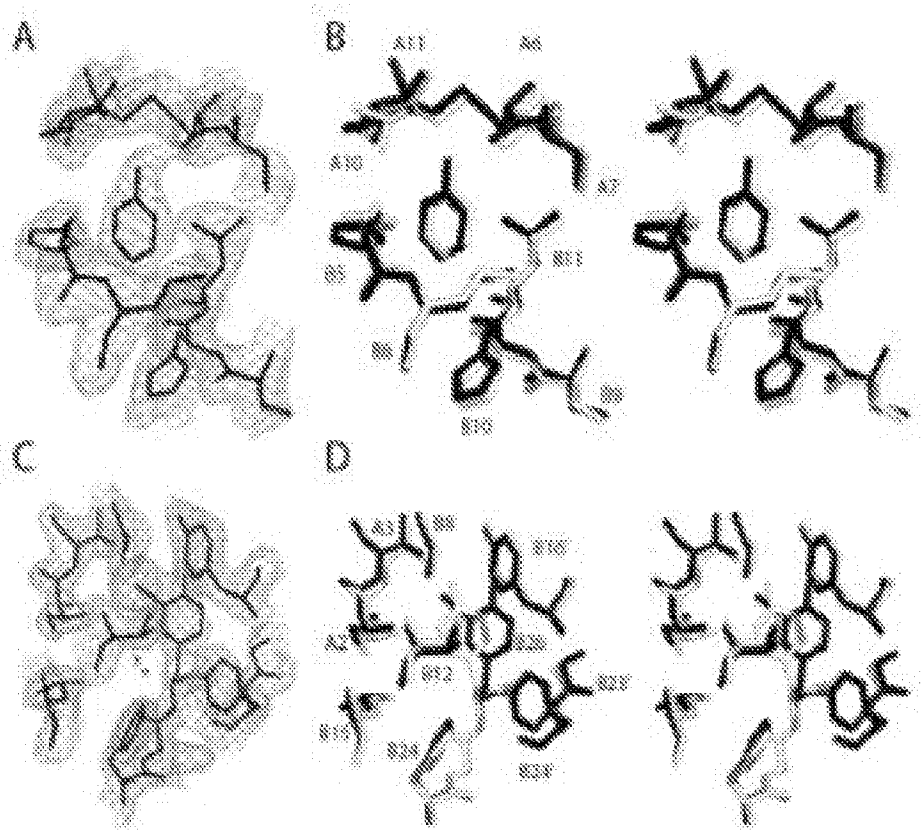

FIG. 7

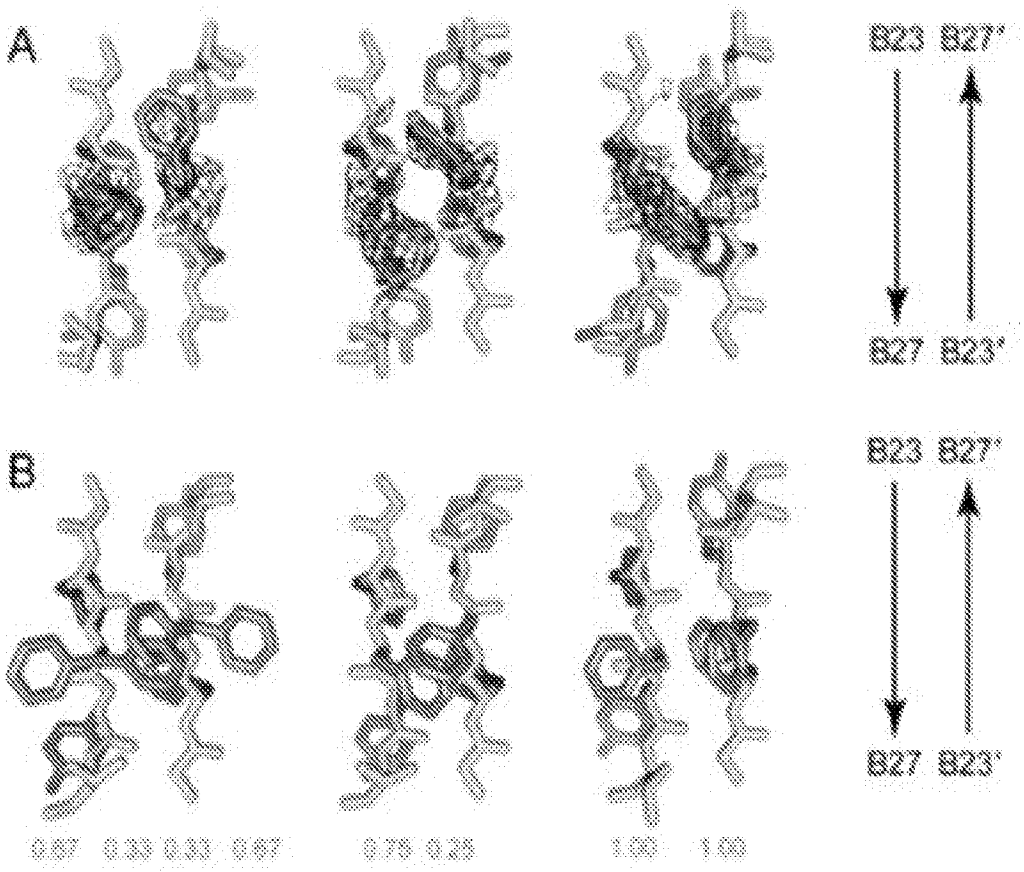
A
B23 B27'
B27 B23'
B
B23 B27'
B27 B23'
0.67 0.33 0.33 0.67
0.75 0.25
1.00 1.00

FIG. 8

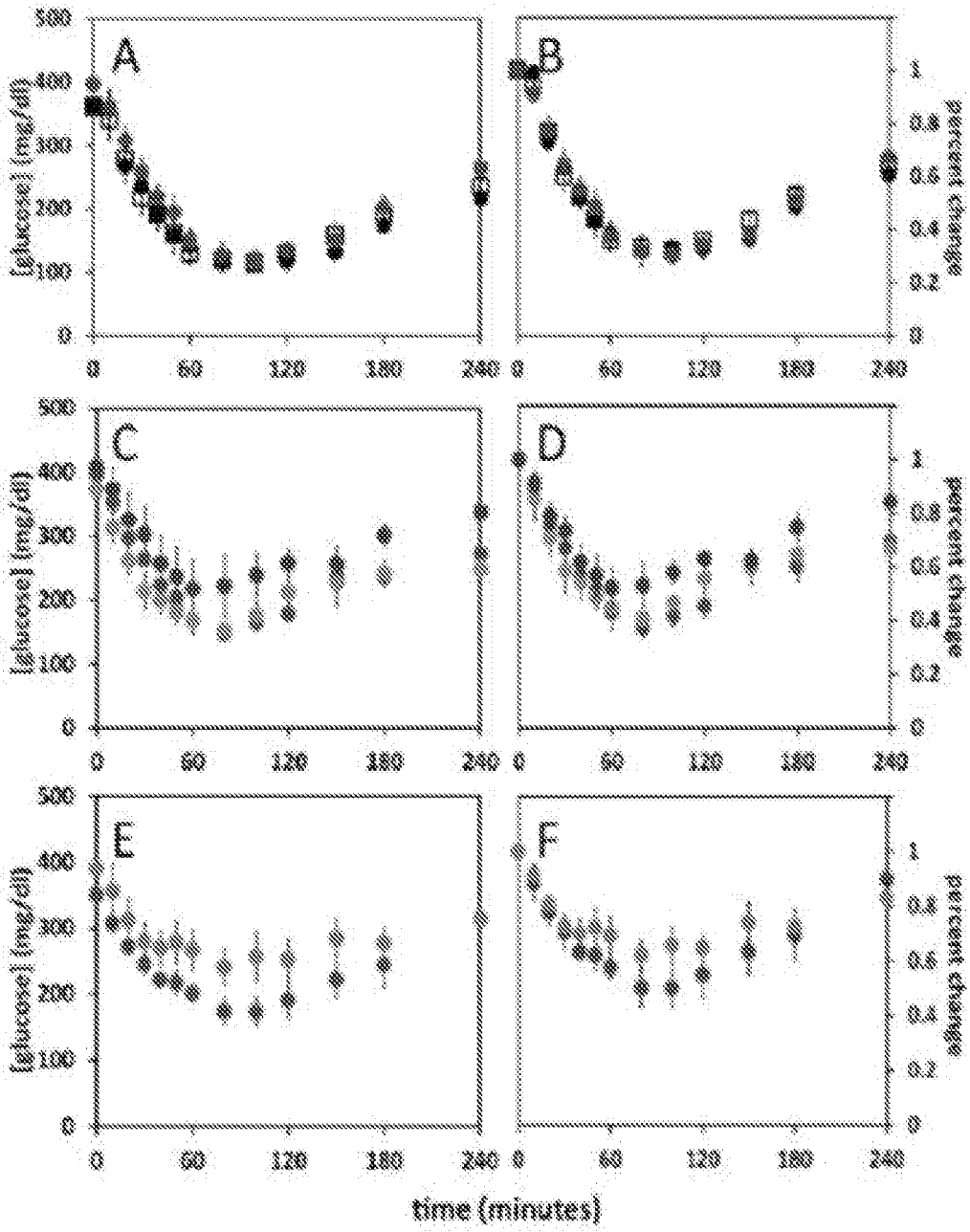
A
B
C
D
E
F
[glucose] (mg/dl)
percent change
time (minutes)
0
60
120
180
240
100
200
300
400
500
0.2
0.4
0.6
0.8
1

FIG. 9

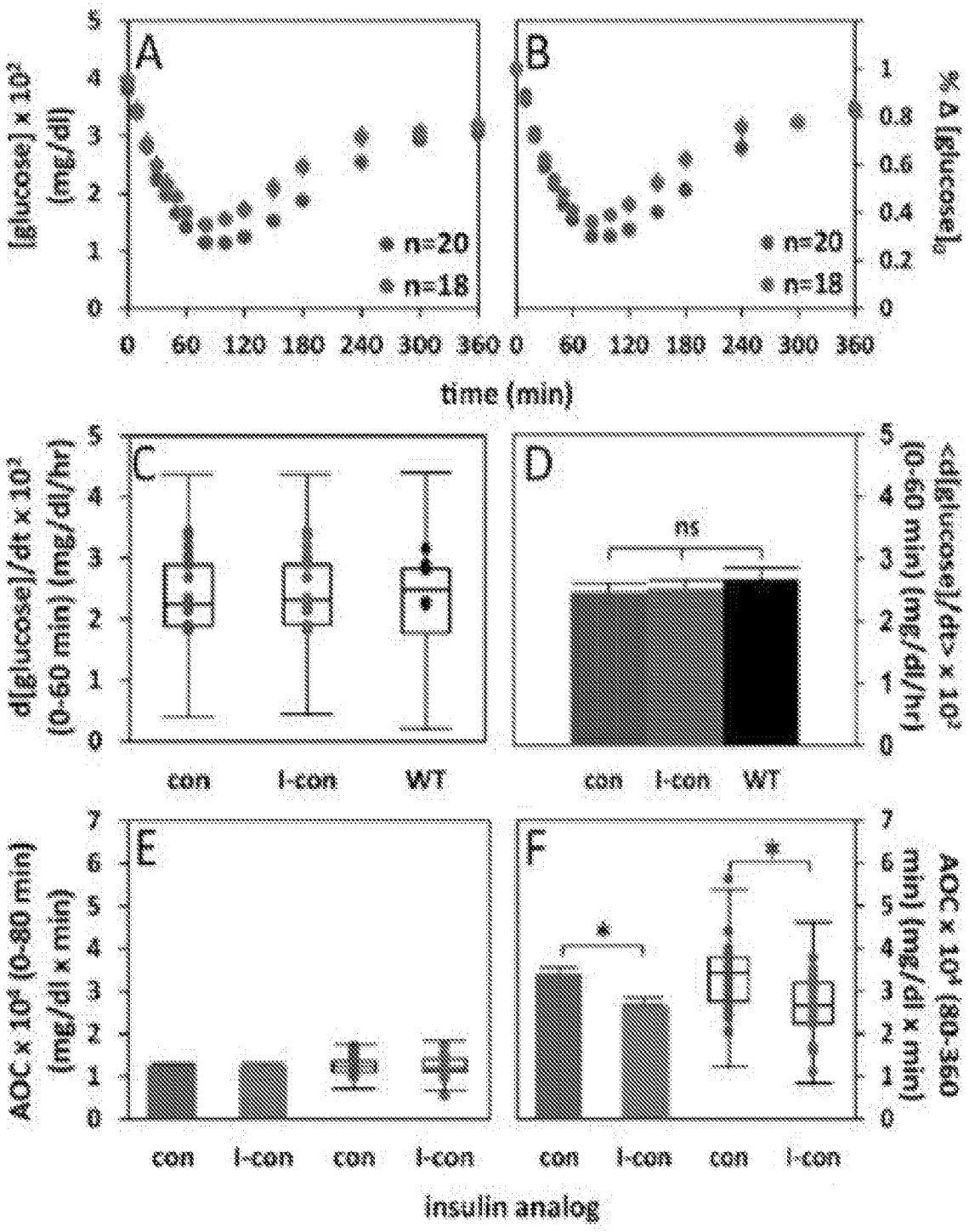
A
B
[glucose] x 10² (mg/dl)
% Δ [glucose]₀
n=20
n=18
0 60 120 180 240 300 360
time (min)
C
D
d[glucose]/dt x 10² (0-60 min) (mg/dl/hr)
<d[glucose]/dt> x 10² (0-60 min) (mg/dl/hr)
ns
con l-con WT
E
F
AOC x 10⁴ (0-80 min) (mg/dl x min)
AOC x 10⁴ (80-360 min) (mg/dl x min)
*
con l-con con l-con
insulin analog

FIG. 10

INTERNATIONAL SEARCH REPORT

International application No.
PCT/US2016/066714

Box No. I Nucleotide and/or amino acid sequence(s) (Continuation of item 1.c of the first sheet)

1. With regard to any nucleotide and/or amino acid sequence disclosed in the international application, the international search was carried out on the basis of a sequence listing filed or furnished:

   a. (means)

   ☐ on paper

   ☐ in electronic form

   b. (time)

   ☐ in the international application as filed

   ☐ together with the international application in electronic form

   ☐ subsequently to this Authority for the purposes of search

2. ☐ In addition, in the case that more than one version or copy of a sequence listing has been filed or furnished, the required statements that the information in the subsequent or additional copies is identical to that in the application as filed or does not go beyond the application as filed, as appropriate, were furnished.

3. Additional comments:

   A sequence listing was filed however it was not used for the purposes of this search and opinion.

INTERNATIONAL SEARCH REPORT

International application No.
PCT/US2016/066714

A. CLASSIFICATION OF SUBJECT MATTER

C07K 14/62 (2006.01) C12N 15/17 (2006.01) C12N 15/63 (2006.01) A61K 38/28 (2006.01) A61P 5/50 (2006.01)

According to International Patent Classification (IPC) or to both national classification and IPC

B. FIELDS SEARCHED

Minimum documentation searched (classification system followed by classification symbols)

Documentation searched other than minimum documentation to the extent that such documents are included in the fields searched

Electronic data base consulted during the international search (name of data base and, where practicable, search terms used)

STN Keyword Search. Files: Medline, Caplus, Wpids, Biosis, Biotechabs. Keywords: INSULIN, PROINSULIN, PRO-INSULIN, B26?, B29?, Iodo?, Iodi?, Weiss.

Applicant/Inventor search in Patentscope/Espacenet/Google. Keywords used: Case Western Reserve University AND Insulin; Weiss AND Insulin.

C. DOCUMENTS CONSIDERED TO BE RELEVANT

Category*	Citation of document, with indication, where appropriate, of the relevant passages	Relevant to claim No.
	Documents are listed in the continuation of Box C	

[X] Further documents are listed in the continuation of Box C

[X] See patent family annex

* Special categories of cited documents:

"A" document defining the general state of the art which is not considered to be of particular relevance

"E" earlier application or patent but published on or after the international filing date

"L" document which may throw doubts on priority claim(s) or which is cited to establish the publication date of another citation or other special reason (as specified)

"O" document referring to an oral disclosure, use, exhibition or other means

"P" document published prior to the international filing date but later than the priority date claimed

"T" later document published after the international filing date or priority date and not in conflict with the application but cited to understand the principle or theory underlying the invention

"X" document of particular relevance; the claimed invention cannot be considered novel or cannot be considered to involve an inventive step when the document is taken alone

"Y" document of particular relevance; the claimed invention cannot be considered to involve an inventive step when the document is combined with one or more other such documents, such combination being obvious to a person skilled in the art

"&" document member of the same patent family

Date of the actual completion of the international search	Date of mailing of the international search report
11 April 2017	11 April 2017
Name and mailing address of the ISA/AU	**Authorised officer**
AUSTRALIAN PATENT OFFICE PO BOX 200, WODEN ACT 2606, AUSTRALIA Email address: pct@ipaustralia.gov.au	Vanessa Williams AUSTRALIAN PATENT OFFICE (ISO 9001 Quality Certified Service) Telephone No. 0262832356

INTERNATIONAL SEARCH REPORT C (Continuation). DOCUMENTS CONSIDERED TO BE RELEVANT		International application No. **PCT/US2016/066714**
Category*	Citation of document, with indication, where appropriate, of the relevant passages	Relevant to claim No.
X	Pandyarajan, V. *et al.*, "Biophysical Optimization of a Therapeutic Protein by Nonstandard Mutagenesis: Studies of an Iodo-Insulin Derivative", The Journal of Biological Chemistry. 2014, vol. 289(34), pages 23367-23381. Table 1; Figure 1; Figure 2	1-6, 8-20
X	Mirmira, R. G. *et al.*, "Importance of the Character and Configuration of Residues B24, B25, and B26 in Insulin-Receptor Interactions", The Journal of Biological Chemistry. 1991, vol. 266(3), pages 1428-1436. Table 1	1, 8-20
X	Frank, B. H. *et al.*, "Receptor Binding properties of Monoiodotyrosyl Insulin Isomers Purified by high Performance Liquid Chromatography", Diabetes. 1983, vol. 32, pages 705-711. Page 710, left-hand column, second paragraph	1, 8-20
P,X	El Hage, K. *et al.*, "Extending Halogen-Based Medicinal Chemistry to Proteins: Iodo-Insulin as a Case Study", The Journal of Biological Chemistry. Published Online 14 November 2016, vol. 291(53), pages 27023-27041. Figure 1, Page 27023, first paragraph.	1-20

INTERNATIONAL SEARCH REPORT Information on patent family members	International application No. **PCT/US2016/066714**

This Annex lists known patent family members relating to the patent documents cited in the above-mentioned international search report. The Australian Patent Office is in no way liable for these particulars which are merely given for the purpose of information.

Patent Document/s Cited in Search Report		Patent Family Member/s	
Publication Number	**Publication Date**	**Publication Number**	**Publication Date**

End of Annex

Due to data integration issues this family listing may not include 10 digit Australian applications filed since May 2001.